Czech Technical University in Prague

Faculty of Electrical Engineering

Doctoral Thesis

February 2015

Petra Píšová

Czech Technical University in Prague
Faculty of Electrical Engineering
Department of Telecommunication Engineering

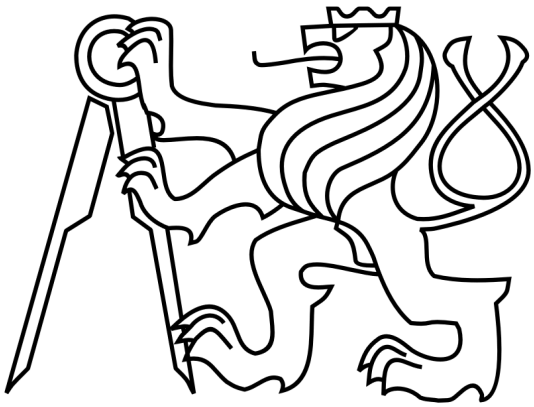

Determination of the Actual User's Position in Urban Environments Using GNSS Multipath Propagation Model

Doctoral Thesis

Ing. Petra Píšová

Ph.D. Programme: Electrical Engineering and Information Technology
Branch of study: Telecommunication Engineering
Supervisor: Doc. Ing. Jiří Chod, CSc.

Prague, February 2015

Thesis Supervisor:

Doc. Ing. Jiří Chod, CSc.
Department of Telecommunication Engineering
Faculty of Electrical Engineering
Czech Technical University in Prague
Technická 2
160 00 Prague 6
Czech Republic

Abstract

This dissertation thesis deals with the problem of reflected GNSS (Global Navigation Satellite System) signals, which are responsible for distorting the information on the actual user position, and with methods on their mitigation and utilization. For decades, GNSSs have been serving well in all areas of human activity. Thanks to augmentation systems, their accuracy is sufficient under usual conditions of the applications. However, the problem arises when the position has to be determined in complex environments, such as narrow streets, mountain valleys etc., where the signal tends to be reflected from various obstacles. This also causes signal delays, thereby distorting the positioning accuracy. This is a very pressing problem in areas such as the navigation for the visually impaired or future navigation of unmanned vehicles.

The main objectives of this thesis are:

- Presenting a theoretical overview of the methods of unwanted signals mitigation.
- Defining and deriving a technique to model complex environments using an intelligent map.
- Proposing a new model of multipath signal propagation in a dynamic environment using the ray-tracing algorithm, 3D building model, known positions of individual satellites acquired from the navigation message, and assumed position of the user.
- Finding a novel method of the determination of the actual user position based on the previous model.

For further specification of contributions and defined objectives of the thesis, see chapter 2.

Keywords:

GNSS multipath propagation, direct signal, reflected signal, 3D building model, built-up area, signal delay estimation, navigation for the visually impaired

Abstract

Disertační práce se zabývá odrazy signálů GNSS (Global Navigation Satellite System - Globální navigační satelitní systémy), které deformují skutečnou polohu uživatele, a metodami vedoucími k jejich potlačení, nebo využití. Globální navigační satelitní systémy dobře slouží již po dlouhá desetiletí ve všech oblastech lidské činnosti. S pomocí podpůrných systémů je jejich přesnost uspokojivá v obvyklých podmínkách aplikací. Problém nastává při požadavcích na přesnost určení polohy ve složitých prostředích, jako jsou úzké ulice měst, horská údolí atd., kde dochází k odrazu signálu od různých překážek, tím i k různému zpoždění navigačního signálu, které pak vede k nepřesnému stanovení polohy uživatele. Tento problém je velmi aktuální např. při určení skutečné polohy pro nevidomé, ale i pro budoucí bezobslužná vozidla.

Hlavním cílem předkládané práce je:

- Poskytnout teoretický přehled metod vedoucích k potlačení vlivu nežádoucích signálů.
- Nalézt a odvodit postup pro modelovaní složitého prostředí pomocí inteligentní mapy.
- Návrh nového modelu k detekci vícecestného šíření signálu v dynamickém prostředí pomocí ray tracing algoritmu, 3D modelu budov, známých poloh jednotlivých družic získaných z navigační zprávy a předpokládané polohy uživatele.
- Nalézt nový způsob zjištěni skutečné polohy uživatele na základě předchozího modelu.

Specifikace definovaných přínosů v podobě cílů disertační práce je uvedena v kapitole 2.

Klíčová slova:

Vícecestné šíření GNSS signálu, přímý signál, odražený signál, 3D model budov, zastavěné území, určení zpoždění signálu, navigace nevidomých

Acknowledgement

I would like to take this opportunity to thank my supervisor Doc. Ing. Jiří Chod, CSc. who inspired me to start the research on GNSS, gave me professional support during the years, and guided me through the process of writing this dissertation.

Table of Contents

List of Figures

List of Tables

Acronyms

ABAS	Aircraft Based Augmentation System
AFI	African Indian Ocean Geographic Region
ALF	Atmospheric Loss Factor
AOA	Angle Of Arrival
AS	Anti-Spoofing
BIH	International Time Bureau / Bureau International de l'Heure
BIPM	International Bureau of Weights and Measures / Le Bureau International des Poids et Mesures
BOC	Binary Offset Carrier
BPSK	Binary Phase Shift Keying
BREP	Boundary Representation
C/A	Course / Acquisition
CDDS	Commercial Data Distribution Service
CDMA	Code Division Multiple Access
CGCS	China Geodetic Coordinate System
CGPM	General Conference on Weights and Measures / Conférence Générale des Poids et Mesures
C/NAV	Commercial Navigation Message
CS	Commercial Service
CTP	Conventional Terrestrial Pole
CTRF	China Terrestrial Reference Frame
DEM	Digital Elevation Model
DGPS	Differential Global Positioning System
DLL	Delay Lock Loop
DOP	Dilution Of Precision
EC	European Commission
ECEF	Earth Centred Earth Fixed
EGNOS	European Geostationary Navigation Overlay Service
EIRP	Effective Isotropic Radiated Power
ESA	European Space Agency
FDE	Fault Detection and Exclusion
FDMA	Frequency Division Multiple Access
FEC	Forward Error Correction
F/NAV	Freely Accessible Navigation Message
FSLF	Free Space Loss Factor

GAGAN	GPS Aided Geo Augmented Navigation (India)
GBAS	Ground Based Augmentation System
GCC	Galileo Control Centre
GCS	Galileo Control System
GDOP	Geometric Dilution Of Precision
GEO	Geostationary Earth Orbit
GGSP	Galileo Geodetic Service Provider
GGTO	GPS to Galileo Time Offset
GIS	Geographic Information System
GLONASS	Global Navigation Satellite System (Russia) / Russian Global'naya Navigatsionnaya Sputnikovaya Sistema
GMS	Galileo Mission System
G/NAV	Governmental Access Navigation Message
GNSS	Global Navigation Satellite System
GPS	United States NAVSTAR Global Positioning System
GTRF	Galileo Terrestrial Reference Frame
HDOP	Horizontal Dilution Of Precision
HOW	Handover Word
IERS	International Earth Rotation and Reference Systems Service
IF	Intermediate Frequency
IGS	International Global Navigation Satellite System Service
I/NAV	Integrity Navigation Message
IRM	IERS Reference Meridian
IRP	IERS Reference Pole
ITRF	International Terrestrial Reference Frame
ITRS	International Terrestrial Reference System
ITU	International Telecommunication Union
KML	Keyhole Markup Language
KMZ	Keyhole Markup Language Zipped
KNIT	Coordination Scientific Information Centre / Koordinatsionity Nautschno - Informatsionity Tsentr
LAAS	Local Area Augmentation System
LHCP	Left Handed Circular Polarization
LO	Local Oscillator
LOS	Line Of Sight
LP	Linear Polarization
MCC	Master Control Centre

MCS	Master Control Station
MEDLL	Multipath Estimating Delay Lock Look
MEO	Medium Earth Orbit
MET	Multipath Elimination Technology
ML	Maximum Likelihood
MMT	Multipath Mitigation Technology
MS	Monitor Station
MSAS	Multi-functional Satellite Augmentation System (Japan)
NASA	National Aeronautics and Space Administration
NAVSTAR	Navigation Satellite Timing And Ranging
NLES	Navigation Land Earth Station
NLOS	Non Line Of Sight
OS	Open Service
P-code	Precision code
PAC	Pulse Aperture Correlator
PDOP	Position Dilution Of Precision
PML	Polarization Mismatch Loss
PNT	Positioning, Navigation, and Timing
PPS	Precise Positioning Service
PRN	Pseudorandom Noise
PRS	Public Regulated Service
PZ90	Earth Parameters 1990 / Parametry Zemli 1990
QPSK	Quadrate Phase Shift Keying
RAG	Receiver Antenna Gain
RAIM	Receiver Autonomous Integrity Monitoring
RCC	Rescue Coordination Centre
RF	Radio Frequency
RHCP	Right Hand Circularly Polarization
RIMS	Ranging and Integrity Monitoring Station
RNAV	Area Navigation
SA	Selective Availability
SACCSA	Augmentation Solution for the Caribbean, Central America and South America / Solución de Aumentación para el Caribe, Centro y Sudamérica
SAR	Search And Rescue
SARSAT	Search And Rescue Satellite Aided Tracking System
SBAS	Satellite Based Augmentation System
SDCM	System of Differential Correction and Monitoring

SNAS	Satellite Navigation Augmentation System (China)
SoL	Safety of Life Service
SPS	Standard Positioning Service
SV	Satellite Vehicle
TAI	International Atomic Time
TDOP	Time Dilution Of Precision
TOW	Time Of Week
UERE	User Equivalent Range Error
US	Upload Stations
UTC	Coordinated Universal Time
UTC(SU)	Coordinated Universal Time (Soviet Union)
UTC(USNO)	Coordinated Universal Time (United States Naval Observatory)
VDOP	Vertical Dilution Of Precision
VSWR	Voltage Standing Wave Ratio
WAAS	Wide Area Augmentation System (United States)
WAD	Wide Area Differential
WADGPS	Wide Area Differential GPS System
WGS84	World Geodetic System 1984

List of Symbols

$\mathbf{A}$	Matrix describing least-squares solution
A	Azimuth
$A_0(t)$	Amplitude of the signal in space
$\mathbf{B}$	Magnetic flux density
$\mathbf{D}$	Electric flux density
$D(t)$	Navigation data
$\frac{\partial \boldsymbol{D}}{\partial \mathrm{t}}$	Displacement current
$\mathbf{E}$	Electric field intensity
E	Elevation
E_l	Parallel component of the electric field
E_r	Perpendicular component of the electric field
$\mathbf{G^T G}$	GDOP matrix
$G_d(t)$	Antenna gain applied to the direct signal
$\mathbf{H}$	Magnetic field intensity
I_i^k	Ionospheric delay
$\mathbf{J}$	Electric current density
$\mathbf{J_f}$	Free current density
$\mathbf{M_{\alpha_1,\alpha_2,\alpha_3}}$	Matrix describing solution to α_1, α_2, α_3
$\mathbf{M_{REF}}$	Matrix describing single reflection
$\mathbf{M_{2\_REF}}$	Matrix describing multiple reflections
$\mathbf{M_{t,s,u}}$	Matrix describing solution to *t, s, u*
P_i^k	Pseudorange
P_{rcv}	Amplitude (received)
P_{tmt}	Amplitude (transmitted)
$P_{x,y,z}$	Receiver position coordinates
R	Distance from the transmitting antenna
$R_{x,y,z}$	Reflection point coordinates
$S_{x,y,z}$	Satellite position coordinates
T_i^k	Tropospheric delay
X_i, Y_i, Z_i	Coordinates of the receiver position
X^k, Y^k, Z^k	Coordinates of the kth satellite position

X_0, Y_0, Z_0	Initial position for the receiver chosen as the centre of the Earth
ΔX, ΔY, ΔZ	Increments updating the approximate receiver coordinates
c	Speed of light
dt_i	Receiver clock offset
dt^k	Satellite clock offset
e_i^k	Observational error of the pseudorange
$\mathbf{e}$	Error vector
f_0	Fundamental frequency
f_d	Doppler shift
f_{IF}	Intermediate frequency
fP	False unexpected position of the receiver
i	Angle of incidence
k	Propagation constant
$\mathbf{n}$	Directional vector
n	Refractive index
$n(t)$	Noise
r	Angle of reflection
$s(t)$	Received signal
t	Input signal at a certain epoch
t_n	Number of leap seconds between GPS system time and UTC time
t_{rcv}	Receiver clock time
t_u	Time bias from GPS system time
$\mathbf{w}$	Normal vector
$x(t)$	Spread spectrum code
$\hat{x}$	Best choice of the system
α	Amplitude attenuation
ϵ	Permittivity
ϵ_0	Vacuum permittivity
θ_1	Incident angle
θ_2	Refracted angle
μ	Permeability
μ_0	Vacuum permeability
ν	Phase velocity

ρ	Volume charge density
ρ_0^k	Range computed from the approximate receiver position
ρ_f	Free charge density
σ_R^2	Ranging variance
τ_0	Arrival time (delay) of the GPS signal
φ	Phase of the plane wave
φ_0	Initial phase
ϕ_d	Phase offset of the direct signal
$\Delta\phi$	Phase shift
$\delta\phi$	Error in the carrier phase measurement due to the multipath
ω	Circular frequency

1 INTRODUCTION

1.1 RESEARCH BACKGROUND

Satellite navigation is based on measuring the delay between signal transmission at the satellite and its reception at a receiver. The measured signal delay is then multiplied by the speed of light – this distance measurement is called the pseudorange. The prefix 'pseudo' is used because these ranges do not correspond to the real geometrical distances to the satellites due to the fact that the receiver time scale is not synchronized to the satellite system time scale and also because the measured signal delays include additional system and propagation errors. To get the user position a technique called trilateration is used [1].

Atmospheric propagation errors (caused by the signal traversing the atmosphere instead of empty space) and multipath errors can be reduced by models or advanced signal processing.

It is well known that multipath is a phenomenon that accounts for a dominant source of error in precise global positioning. In dynamic urban environment, it changes rapidly so it is difficult to detect, predict, and control.

Generally, direct (or line-of-sight) signal is normally the most wanted signal. Nevertheless, signals can also arrive at the receiver via a number of different paths that may occur between the satellite and the receiver. These paths are results of reflections and diffractions from buildings of different heights, structures, and materials – reducing the number of visible satellites and thus increasing the presence of multipath.

Typically, an antenna receives the direct signal and one or more of its reflections. The reflected signal is usually a weaker version of the direct signal which takes more time to reach the receiver than the direct signal. This path delay, or rather this difference between the length of the path taken by the reflected signal and the direct signal itself (between the satellite and the receiver) causes an important pseudorange measurement error. Reception of reflected signals also causes distortion in the code correlation peak within the receiver. Therefore, the code phase of the direct signal cannot be determined precisely.

Typical multipath error in pseudorange measurements ranges from 1 m (in a fair environment) to over 5 m (in highly reflective environment) and the phase measurement error does not exceed a quarter cycle (if the reflected signal is of a smaller amplitude than the direct signal) [2].

It is difficult to mitigate the multipath by models, because it depends strongly on users' local environment – the influence of given signal and receiver parameters on the actual

multipath error depends on various factors. Different multipath mitigation techniques have been developed to improve positioning performance in built up areas. In general, they can be grouped into three main categories: antenna-based, receiver-based, and post receiver-based techniques. Many are used in combination; however, multipath mitigation still remains a hot topic of research [3].

Analysing different combinations of Global Navigation Satellite Systems (GNSS) constellations promises more considerable improvements than mere analysing data from a single GNSS constellation. There are several satellite systems in operation today, such as the United States NAVSTAR Global Positioning System (GPS) or the Russian GLONASS (Global'naya Navigatsionnaya Sputnikovaya Sistema). Chinese Compass navigation system and the European Union's Galileo navigation system are currently under construction.

Three-dimensional (3D) reconstruction and texturing of buildings is becoming increasingly important for a number of applications and has been a topic of active research in recent years. As 3D building models are becoming more geometrically accurate, they can be regarded as new true data sources which can improve positioning accuracy in urban canyons.

Therefore, one promising solution is to use known positions of the satellites extracted from a navigation message in combination with 3D building models and known position of the user. These quantities may help to calculate the path lengths of direct signals and even path delays of reflected signals and thus to predict blockage and reflection of GNSS signals. This approach can be then used to estimate the subject's unknown position while moving in the same environment.

1.2 DISSERTATION OUTLINE

The remainder of the thesis is organized as follows:

Chapter 2

Chapter 2 describes the aims of the thesis.

Chapter 3

Chapter 3 focuses on standing multipath mitigation techniques. In general, they are grouped into three main categories: antenna-based, receiver-based, and post receiver-based techniques and their combinations.

Chapter 4

Chapter 4 presents the Global Navigation Satellite Systems (GNSSs), their classification, system, signal overview, and navigation message structure.

Chapter 5

Chapter 5 gives a brief overview of existing GNSS augmentation systems capable of improving the accuracy, integrity, and availability of GNSS systems.

Chapter 6

Chapter 6 explains different reference frames and internal reference time scales used in GNSS for their positioning and timing solution.

Chapter 7

Chapter 7 describes the electromagnetic wave properties and changes the GNSS signal goes through on the path from a satellite to a receiver.

Chapter 8

Chapter 8 classifies received signals into three main types: direct signals (line-of-sight, LOS), indirect signals (non-line-of sight, NLOS), and blocked signals. It also introduces a set of indirect signal characteristics that are different from those of directly received signals.

Chapter 9

Chapter 9 provides an overview of standard GNSS antennas and receivers functions.

Chapter 10

Chapter 10 defines main GNSS sources of error.

Chapter 11

Chapter 11 lays out the methodology of 3D environment model preparation: obtaining 3D geometry data from real environment, extracting them into 3D modelling software, determining current satellites visibility above the user's receiver, and transforming their coordinates into the in mapping coordinates.

Chapter 12

Chapter 12 defines a research model used for multipath detection in dynamic propagation environments. The model is based on ray tracing algorithm.

Chapter 13

Chapter 13 shows how to use the previous approach to determine the unknown position while moving in the same dynamic environment using the interval halving method.

Chapter 14

Chapter 14 includes a call detailed graph including software functions and their description – MATLAB code can be found on the supplemented CD attached to the inside back cover.

Chapter 15

Chapter 15 provides results of the experiments.

Chapter 16

Chapter 16 includes general conclusions and discussion.

2 AIMS OF THE THESIS

Global navigation satellite systems (GNSS) have been in operation for several decades. They affect virtually all areas of human activity. Thanks to augmentation systems (involving correction of signal propagation in the ionosphere and differential measurements at referential points), their accuracy – typically about 1 m – is satisfactory under usual conditions of their applications. The problem arises when the position needs to be determined in complex environments, such as narrow town streets, mountain valleys etc., where the signal tends to be reflected from various obstacles. This causes signal delays, thereby distorting user positioning accuracy. Depending on the nature of the environment, the deviation may amount up to tens or hundreds of meters. This system deficiency is not necessarily fatal in today's situation when cars are operated by drivers. In this case, some deficiencies can be corrected, e.g. by software combination of the data with the information on a navigation route and by estimation of the real position by a driver. However, the situation changes dramatically in case of unmanned, self-driving vehicles. Although these are not very common yet, this era is fast approaching. This problem is also very pressing in other areas where the exact position needs to be determined, such as in precise data processing within the navigation for the visually impaired.

There are many methods to counter these problems. The simplest approach is based on the knowledge of the fact that polarization of a GNSS signal changes upon reflection (from right-handed to left-handed and vice versa). There is thus an option to consider only those signals which did not undergo this change. For this purpose, antennas suppressing unwanted (i.e. unsuitably polarized) signals may be used. Similarly, it is possible to determine the actual segment of the sky situated above a receiver which contains only directly "visible" satellites. This may be done using intelligent maps which contain data on the location and height of surrounding objects. While the first method is already commonly available, the other – map-based computation – is currently not widely used as it is very demanding of computing power of the receiver processor. Moreover, the number of satellites situated in direct line of sight is usually not sufficient so the position cannot be determined with satisfactory accuracy.

Other, statistics-based, techniques try to calculate the relevant data. Methods based on so-called Maximum Likehood Estimation (MLE) are being tested, such as Multipath Estimation Delay Lock Loop (MEDLL), Fast Iterative Maximum-Likelihood Algorithm (FIMLA), Multipath Mitigation Technology (MMT), and Vision Correlator (VC) among others (see the overview included in the thesis). Nonetheless, methods of this sort are very demanding mathematically so it is very difficult to implement them.

All these methods discovered so far do show some results but remain inadequate for the time being. Moreover, these procedures usually demand the use of highly specialized, high-cost, relatively low-efficient receivers.

I have therefore decided to design a new technique which is based on the fact that intelligent maps (i.e. those which contain information on the height of surrounding objects and possibly other relevant data, such as the nature and structure of the surface) are relatively easily available today and they can be used to determine the actual position by calculating signal reflections and their comparison with the data measured by a navigation receiver.

The main task is thus finding a computing model which would be able to provide the information on reflected signals from navigation satellites (because their position at any point in time is known with sufficient accuracy). If we know the expected situation of direct versus reflected signals at a defined location, then it is also possible to reverse the procedure and to look for the actual position of a GNSS user by means of the comparison of the measured and calculated data.

This is done using the interval halving method in several (typically three to five) steps until the difference between the calculated and measured data is acceptable.

The dissertation objectives are thus as follows:

1. An analysis of the environment and the movement of a GNSS user within the area of interest.
2. Determining the anticipated route of the GNSS user, including the definition of deviation tolerance intervals.
3. In case of a mismatch between the position measured by the GNSS and the anticipated route, determining the number of directly visible satellites. If the number of satellites is not sufficient (fewer than four), determining the starting point and the endpoint of the route in the area of interest.
4. Computation of a 3D-object model using an intelligent map, taking into account the data on positions of all available satellites situated above the horizon.
5. Setting the beginning of the computation of signals and their reflections to the midpoint of the route (a point halfway between the starting point and the endpoint as defined in point 3).
6. Computation of the signals and their reflections using the model.
7. Depending on the contrast between the position computed and data measured, a consequent decision which half of the route is relevant, then moving the next step of the computation to the midpoint of this segment.

8. Another round of signal computation for the new position and displaying the result (i.e. repeating point 6).
9. Repeating point 7 in subsequent steps until the difference between the measured and computed positions lies within the desired tolerance interval.
10. Marking the last computed position as the actual position.

It is evident that a crucial prerequisite is creating a digital terrain model related to the position of the satellites and determining the reflections of their signals in the defined position of the user. And it is precisely this condition, i.e. creating the model and necessary algorithms, what is the focal point of my dissertation thesis.

3 CURRENT SITUATION OF THE STUDIED PROBLEM

It is difficult to mitigate multipath by models, because it strongly depends on user's local environment [1].

Influence of given signal and receiver parameters on the actual multipath error depends on various factors [4]:

- code chipping rate;
- signal-type modulation;
- pre-correlation bandwidth and filter characteristics;
- number of received multipath signals;
- relative power of multipath signals;
- path-delay;
- chip spacing between correlators;
- type of discriminator and algorithm used for code and carrier frequency tracking.

Different techniques exist to mitigate the effect of multipath signals. In general, they can be grouped into three main categories: antenna-based, receiver-based, and post receiver-based techniques. Many are used in combination [3].

3.1 ANTENNA-BASED MITIGATION TECHNIQUE

As mentioned above, GNSS signals are right-hand circularly polarized (RHCP), while most reflected signals show left-handed circular polarization (LHCP) or mixed polarization. The signal, however, remains RHCP when the angle of incidence is greater than the Brewster's angle. Brewster's angle varies with different reflective surfaces [5]. A RHCP antenna is able to supress the LHCP reflection quite effectively too and minimize (but not entirely remove) the multipath reflection error.

Therefore, the principle applied in GNSS antennas means increasing the sensitivity for RHCP and simultaneously decreasing the sensitivity of LHCP signals: A well-designed GNSS antenna is at least 10 decibels more sensitive to RHCP signals than LHCP signals at normal incidence in order to decrease the magnitude of the code and carrier tracking errors due to multipath appearance. The exception is the case of low elevation signals, for which the antenna has very little polarization discrimination. To attenuate low and negative elevation signals, modern design uses variable choke-ring antennas (depending on space permits) [3].

A space-effective alternative is the use of the dual-polarization antenna technique which correlates the right hand circularly polarized (RHCP) and left hand circularly polarized (LHCP) outputs separately. If an LHCP C/N_0 is larger than the corresponding RHCP C/N_0, the multipath interference is detected. This is not effective for low elevation signals [6].

Another technique is the use of a GNSS antenna array to estimate the angle of arrival (AOA) of incoming GNSS signals [3]. For multipath and directly received signals determination, measured lines of sight are compared with data predicted from the satellite ephemeris. This method is used for detecting strong multipath interference.

An advanced method is special processing that uses directive antenna arrays to provide required directive pattern with high gain in the direction of the direct signal and attenuation from directions of reflected signals [7]. Directive antennas are not affordable for most civilian applications because they are usually physically large and heavy [3].

3.2 RECEIVER-BASED MITIGATION TECHNIQUE

There are many techniques to mitigate the effects of multipath on pseudorange measurements by increasing the resolution of the receiver's code discriminator, and thus separating the direct signal from the reflected signal components [3].

Examples of recently developed in-receiver multipath mitigation techniques are:

- narrow correlator;
- double-delta discriminator;
- gated and high resolution correlator;
- multipath-estimating delay lock look (MEDLL);
- vision correlator;
- strobe and edge correlator;
- enhanced strobe correlator;
- multipath elimination technology (MET);
- multipath mitigation technology (MMT);
- maximum likelihood (ML) estimator;
- pulse aperture correlator (PAC;
- early1/early2 (E1/E2) tracking technique.

Superior methods like MEDLL, MMT, and VC rely on maximum likelihood (ML) estimation principles. However, they are typically complex and difficult to implement as they require cross-correlation function for each reflected path with multiple correlators to measure the received signal and to process these measurements with complex algorithms [4].

3.3 POST RECEIVER-BASED MITIGATION TECHNIQUE

Multipath effects on code and phase measurements differ extensively. Multipath also creates different errors on different frequencies, it can be therefore detected and mitigated by comparing different measurements of signals on different frequencies from the same satellite [8] – an example is carrier smoothing to reduce code multipath errors for dynamic applications [3].

Another method is signal selection based on consistency checking: the position is computed using measurements from different satellites that are compared with each other to identify reflected signals. The same principle is used for fault detection in receiver autonomous integrity monitoring (RAIM) where algorithms require at least five visible satellites to detect the presence of a large position error [9].

High performance positioning is also achieved by using Kalman filter where inconsistent measurements are determined by using information from previous epochs.

Research done in this work

One promising solution is to make use of multiple satellite constellations along with the combination of 3D building models and known position of the user to calculate the path length of direct signals or rather the path delay of reflected signals and thus to eliminate multipath impact on the position. This method is theoretically possible but requires a very accurate model allowing simulating a realistic propagation of the GNSS signal.

Further information on multipath interference may be found in standard GNSS books [3].

4 GNSS

Global Navigation Satellite Systems (GNSS) is a standard term for all kinds of satellite navigation systems that provide real time positioning and velocity determination with global coverage.

Today, the only fully developed and globally operational GNSS are the United States NAVSTAR Global Positioning System (GPS) and the Russian Global'naya Navigatsionnaya Sputnikovaya Sistema (GLONASS). Chinese regional BeiDou navigation system is also being expanded into the global Compass navigation system while the European Union's Galileo navigation system is currently in the deployment phase, both services expected to be fully operational by 2020 at the earliest.

GNSS can be classified as follows [10]:

- GNSS-1 is the first generation of navigation systems including GPS, GLONASS, and Satellite Based Augmentation Systems (SBAS) or Ground Based Augmentation Systems (GBAS);
- GNSS-2, a result of an extension of civil and military demands, is the second generation of navigation systems currently being developed. It includes a modernization of GPS, achieving full global coverage of GLONASS, building new European Galileo navigation system designated for civil purposes, and also building Chinese Compass to provide global navigation services. All these main navigation systems can also be combined with SBAS and GBAS augmentation systems.

Once all these GNSSs become fully operational and receivers are able to process multiple navigation systems, the GNSS-2 advantages will be enormous.

4.1 GPS

The Global Positioning System (GPS) is a US-owned system that provides users with positioning, navigation, and timing (PNT) services. While there are many thousands of civil users of GPS worldwide, the system was primarily designed for and is operated by the US Air Force [11], [12].

4.1.1 System Overview

The system consists of three segments: the space segment, the control segment, and the user segment.

SPACE SEGMENT

To provide worldwide three-dimensional navigation, the space segment consists of six orbital planes, requiring a minimum of four satellites in each.

The satellites fly in Medium Earth Orbit (MEO) at an altitude of approximately 20,200 km and are inclined to the equator by 55°. The satellites have a period of 12-hour sidereal time which means that they circle the Earth twice a day. Each satellite simultaneously transmits a ranging signal that includes its navigation message with current position and time correction information [11].

CONTROL SEGMENT

The GPS control segment consists of five monitoring stations (located at Hawaii, Kwajalein, Ascension Island, Diego Garcia, and Colorado Springs), three ground antenna upload stations (located at Ascension Island, Diego Garcia, and Kwajalein), and the Master Control station located at Schriever AFB in Colorado [11].

The main objective of the GPS Control Segment is to maintain each satellite in its proper orbit, make corrections to the satellite clocks, and generate and upload navigation data to the satellites.

USER SEGMENT

As there are many GPS applications for military and civil purposes, there are also many different GPS receivers with different modes of operation – such as airborne GPS receivers, land mobile navigation receivers, marine navigation receivers, differential GPS (DGPS), GPS survey, and hybrid GPS receivers.

The main purpose of a receiver is to track the ranging signals of selected satellites and calculate three-dimensional position and local time.

4.1.2 GPS SIGNAL OVERVIEW

GPS satellites generate and transmit three radio frequencies in the L-band (1000 to 2000 MHz of the radio spectrum), all derived from the fundamental frequency f_0 (10.23 MHz) of the satellite oscillator [13], [14]:

- L1 = 1575.42 MHz = 154*f0 = 154*10.23 MHz; (4. 1)
- L2 = 1227.6 MHz = 120*f0 = 120*10.23 MHz; (4. 2)
- L5 = 1176.45 MHz = 115*f0 = 115*10.23 MHz. (4. 3)

All carrier signals are modulated by the navigation message and also by the pseudorandom codes (PRN) using the binary phase shift keying (BPSK) modulation, the

binary offset carrier (BOC) modulation, or the quadrate phase shift keying (QPSK) modulation.

The L1 signal is modulated by the course/acquisition code (C/A code) and by the precision code (P-code). The L2 signal is modulated either by the P-code or by the C/A code [2], [15]. The chipping rate of the C/A code is $1.023*10^6$ chips/sec ($f_0/10$ = 1.023 MHz), similarly for the P-code $10.23*10^6$ chips/sec (f_0 = 10.23 MHz). The C/A code was designed for civilians using the Standard Positioning Service (SPS), whereas the P-code for military purposes using the Precise Positioning Service (PPS). Generally, the P-code is restricted to the SPS users if so called antispoofing mode (AS) is activated at the satellite – this technique modulates an encryption on the P-code and produces the Y-code, that is, the P(Y) code [15].

Two PRN codes are transmitted on L5: the in-phase code (termed I5-code) and the quadrature-phase code (termed Q5-code). The chipping rate for both codes is $10.23*10^6$ chips/sec (f_0 = 10.23 MHz). The I5-code is modulated with a 10-bit Neuman-Hofman code and the Q5-code is modulated with a 20-bit Neuman-Hofman code [16], both clocked at 1 kHz.

The GPS signals use the Code Division Multiple Access (CDMA) technique which allows each satellite to transmit a unique PRN code on the same frequency.

Ending Selective Availability

Selective Availability (SA) used to be a purposeful reduction of civilian GPS accuracy, implemented on worldwide basis through its satellites for the reasons of national security. In May 2007, the SA feature was deactivated in order to make GPS more responsive to civil and commercial users. In 2007, it was decided that the future generation of GPS satellites (termed GPS III) will be built without the SA [11].

4.1.3 NAVIGATION MESSAGE STRUCTURE

4.1.3.1 NAVIGATION MESSAGE FORMAT

The GPS message consists of frames, sub-frames, and words. The basic format is a 1500-bit long frame. Each frame is composed of five sub-frames with the length of 300 bits. Each sub-frame contains ten 30-bit words. Sub-frames 1, 2, and 3 are repeated in each frame. However, sub-frames 4 and 5 consist of 25 pages each.

At the rate of 50 bps, the transmission time of one frame lasts 30 s, which means just 6 s per sub-frame. Transmitting one entire navigation message (37,500 bits of data) takes 12.5 minutes [13], [17].

4.1.3.2 NAVIGATION MESSAGE CONTENT

The sub-frames transmit following data [9]:

- Sub-frame 1: GPS week number, SV accuracy and health, and clock correction terms;
- Sub-frames 2–3: satellite ephemeris parameters;[1]
- Sub-frame 4: almanac and health data for SVs 25–32, special messages, satellite configuration flags, and ionospheric and UTC data;
- Sub-frame 5: almanac and health data for SVs 1–24, almanac reference time, and the week number.

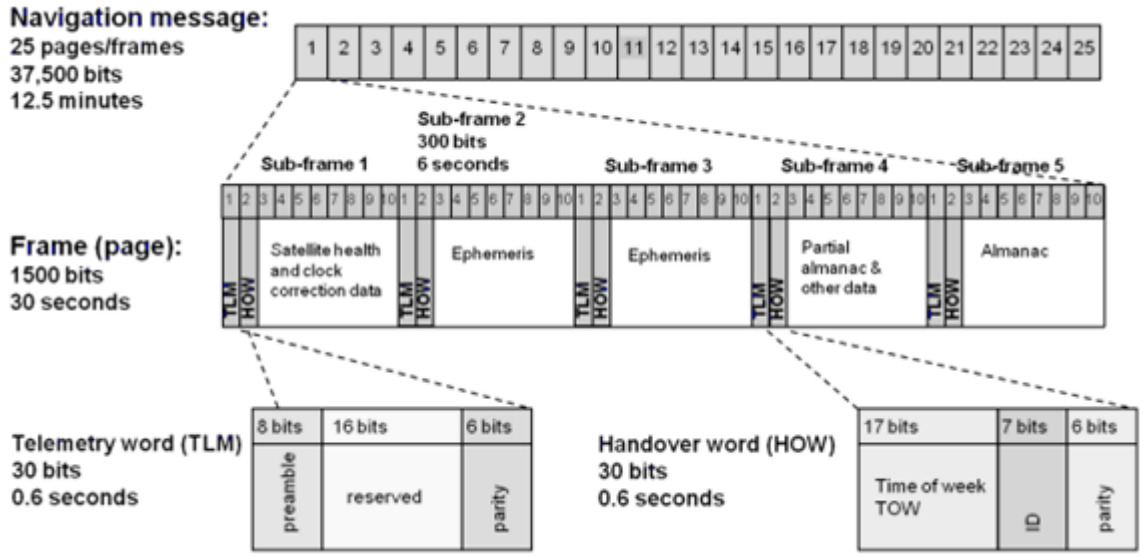

Figure 4. 1 GPS navigation message structure [18]

At the beginning of each sub-frame (bits 1-60), there are two special words, telemetry data (TML) and a handover word (HOW).

The GPS telemetry word (TLM) is 24 bits long. It is used to provide the start information for the sub-frame (data synchronisation). It is repeated every 6 s and it changes just when uploading. It contains a fixed 8-bit preamble followed by a 16-bit message including reserved bits and parity.

The GPS handover word (HOW) contains a 17-bit long information of the Time of Week (TOW - used for time synchronization), an anti-spoofing flag, a reserved alert flag (used to indicate a poor signal accuracy), sub-frame identification information, and parity checking bits. It changes every 6 s [9].

[1] Each satellite transmits almanac data for all GPS satellites, but it only transmits ephemeris data for itself [17].

4.2 GLONASS

GLONASS (Global'naya Navigatsionnaya Sputnikovaya Sistema) is managed for the Russian Federation Government by the Russian Space Forces and the system is operated by the Coordination Scientific Information Centre (KNITs) of the Ministry of Defence of the Russian Federation [19].

4.2.1 System Overview

The system consists of three segments: the space segment, the control segment, and the user segment.

Space Segment

The GLONASS space segment consists of 21 satellites in three orbital planes, with three on-orbit spare ones. The three orbital planes are separated by 120°, the satellites within the same orbit plane by 45°. Each satellite operates in circular 19,100 km orbits at an inclination angle of 64.8° where each satellite completes an orbit in approximately 11 hours 15 minutes.

Control Segment

The ground control segment of GLONASS is entirely located within the territory of former Soviet Union. The Ground Control Centre and Time Standards are located in Moscow whereas the telemetry and tracking stations are located at St. Petersburg, Ternopol, Eniseisk, and Komsomolsk-na-Amure.

User Segment

The User Segment consists of receivers that track and receive satellite signals. They must be capable of simultaneous processing the signals from a minimum of four satellites to obtain accurate position, velocity and timing measurements. Like GPS, GLONASS is both a military and a civilian-use system [19].

4.2.2 GLONASS Signal Overview

The GLONASS satellites generate and transmit frequencies in the L-band, all derived from the fundamental frequency f_0 (10.23 MHz) of the satellite oscillator [14].

For the L1-band and L2-band, the GLONASS signals use the Frequency Division Multiple Access (FDMA) technique which allows each satellite to transmit the same code on a different frequency:

- The nominal carrier frequencies of the L1 signals: 1602 MHz + n × 0.5625 MHz; (4. 4)
- The nominal carrier frequencies of the L2 signals: 1246 MHz + n × 0.4375 MHz; (4. 5)

where n is a satellite's frequency channel number (n = -7 .. +6).

Since the GLONASS frequencies in the band 1610.6 – 1613.8 MHz interfere with frequencies used for radio astronomical observations, the band was closed and all GLONASS satellites launched since 2005 now use channels n=-7 to +6, with channels +5 and +6 used only for orbital insertion (GLONASS-ICD 2002) [14].

For the sake of compatibility with GPS and Galileo signals, the GLONASS signal structure is in the process to use the Code Division Multiple Access (CDMA) technique in the existing L1, L2 signals and new for L3 and L5 signals. The open signal L3 is centered at 1202.25 MHz, using the quadrate phase shift keying (QPSK) modulation. It is planned to be launched in 2015. The future L5 signal is planned to be centered at 1176.45 MHz. It is planned to be launched by 2025.

The GLONASS signals use the binary phase-shift keying (BPSK) modulation, the binary offset carrier (BOC) modulation, and the quadrate phase shift keying (QPSK) modulation. GLONASS transmits C/A-code and P-code. Similarly to GPS, the chipping rate of the C/A code is $1.023*10^6$ chips/sec ($f_0/10 = 1.023$ MHz), as for the P-code $10.23*10^6$ chips/sec ($f_0 = 10.23$ MHz).

4.2.3 NAVIGATION MESSAGE STRUCTURE

4.2.3.1 NAVIGATION MESSAGE FORMAT

In a similar way to the GPS, the GLONASS navigation message is composed of super-frames, frames, and strings. Each super-frame contains five frames and has duration of 2.5 minutes. Each frame contains 15 strings and takes 30 seconds to transmit.

The navigation message[2] includes immediate and non-immediate data transmitted at 50 bps [20].

4.2.3.2 NAVIGATION MESSAGE CONTENT

Within each super-frame, a total content of non-immediate data (almanac for 24 satellites) and the immediate data (for the satellite being tracked) is transmitted.

Each frame consists of 15 strings, each of duration of two seconds. Data in the first four strings of each frame contain the immediate data related to the satellite transmitting the navigation message (ephemeris data, clock corrections, health status, and frequency information). The immediate data are the same for all the frames in a super-frame. Strings 6–15 of each frame include non-immediate data for all 24 satellites. Frames 1–4 contain non-immediate data for 20 satellites while the 5th frame contains the non-immediate data for

[2] Navigation message for high precision signal has not been officially published [18].

the remaining 4 satellites. Non-immediate data for each satellite occupy two strings. Data contained in the 5th string of each frame are the same in one super-frame. They relate to the non-immediate data [20].

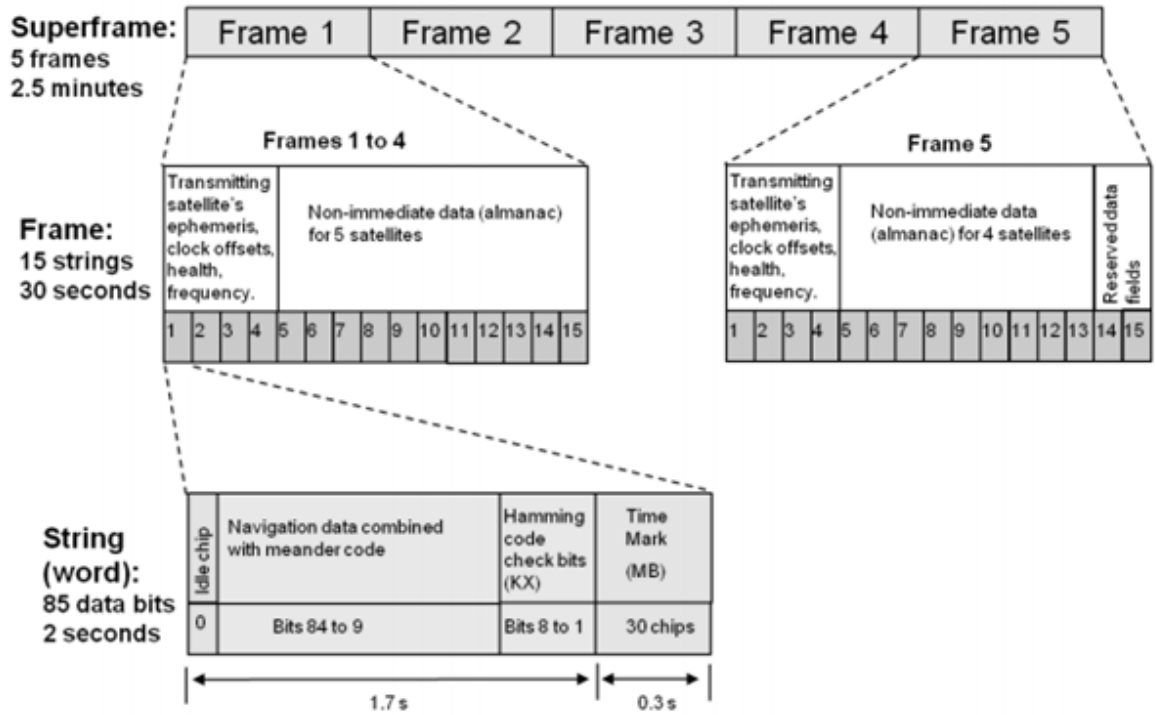

Figure 4. 2 GLONASS navigation message structure [18]

Each string lasts 2 seconds. During the first 1.7 seconds, 85 bits of data are transmitted (i.e. modulo-2 addition of 50 Hz navigation data and 100 Hz auxiliary meander sequence). During the remaining 0.3 seconds, a time mark (shortened pseudo random sequence) is transmitted. Along with data bits (bit positions 9–84), the check bits of Hamming code (bit positions 1–8) are transmitted. The data of one string are separated from the data of the adjacent strings by a time mark (MB). The last bit in each string (bit position 85) is an idle chip (0). It serves for realization of sequential relative code when transmitting the navigation data via a radio link (GLONASS ICD 2002) [21].

4.3 GALILEO

Galileo is Europe's own global navigation satellite system which is to provide a highly accurate, guaranteed global positioning service under civilian control. Galileo is a joint initiative of the European Commission (EC) and the European Space Agency (ESA) [22].

4.3.1 SYSTEM OVERVIEW

The system consists of three segments: the space segment, the control segment, and the user segment.

SPACE SEGMENT

As soon as Galileo is fully operational, there will be 30 satellites in Medium Earth Orbit (MEO) at an altitude of 23,222 kilometres. Ten satellites will occupy each of three orbital planes inclined at an angle of 56° to the equator. The satellites will be spread evenly around each plane and will take about 14 hours to orbit the Earth. One satellite in each plane will be a spare [22].

CONTROL SEGMENT

The Ground Segment will comprise two control centres (GCC). Each control centre will manage control functions (supported by the dedicated Galileo Control System (GCS) located in Oberpfaffenhofen Control Centre in Germany) and mission functions (supported by a dedicated Galileo Mission System (GMS) located in the Fucino Control Centre in Italy). The GCS will handle spacecraft housekeeping and constellation maintenance while the GMS will handle the control over the navigation system [22].

USER SEGMENT

The User Segment consists of receivers that receive Galileo signals, determine pseudoranges, solve the navigation equations in order to obtain their coordinates, and provide accurate time information [22].

4.3.2 GALILEO SIGNAL OVERVIEW

Just as in GPS and GLONASS, Galileo signals are derived from the fundamental frequency f_0 (10.23 MHz) of the satellite oscillator. All Galileo satellites will transmit signals on three different frequencies using the code division multiple access (CDMA) technique:

- E1 = 1575.42 MHz; (4. 6)
- E6 = 1278.75 MHz; (4. 7)
- E5a (L5) = 1176.45 MHz; (4. 8)
- E5b = 1207.140 MHz. (4. 9)

The Galileo signals will use the binary offset carrier (BOC) modulation and the quadrate phase shift keying (QPSK) modulation [23]. Altogether, Galileo will provide five levels of services [24]:

- The Open Service (OS) signals will use unencrypted ranging codes and unencrypted navigation data messages on the E5a, E5b, and E1 carriers.

- The Safety-of-Life Service (SoL) signals will use the OS ranging codes and navigation data messages on E5a, E5b, and E1 carriers.

- The Commercial Service (CS) signals will use the OS ranging codes and navigation data messages, possibly with additional CS encrypted data messages on the E5b carrier and may also use an encrypted CS ranging code and navigation data messages on the E6 carrier.

- The Public Regulated Service (PRS) signals will use the encrypted PRS ranging code and navigation data messages on the E6 and E1 carriers.

- As a new feature compared to GPS and GLONASS, Galileo will provide a global Search and Rescue (SAR) function, based on the operational COSPAS-SARSAT (Cosmicheskaya Systyema Poiska Avariynyich Sudov - Search And Rescue Satellite Aided Tracking) system. Each Galileo satellite will be able to transfer distress signals from users' transmitters to the Rescue Coordination Centre, which will then initiate a rescue operation. At the same time, the system will inform the user that the help is under way [14].

4.3.3 NAVIGATION MESSAGE STRUCTURE

4.2.3.1 NAVIGATION MESSAGE FORMAT

Depending on the service and signal content, Galileo will transmit four different navigation messages [25]:

- Freely Accessible Navigation (F/NAV) message – contains navigation data only;
- Integrity Navigation (I/NAV) message – contains navigation, SAR, integrity and service management data;
- Commercial Navigation (C/NAV) message – contains service management data;
- Governmental Access Navigation (G/NAV) message – contains navigation, integrity, and service data for PRS.

The Galileo navigation message format for the E1 open service is referred to I/NAV and has a fixed form. It contains frames, sub-frames, and pages similar to those in GPS and GLONASS.

A frame consists of 24 sub-frames and is 720 seconds long. Each sub-frame contains 15 pages and lasts 30 seconds. Each page takes 2 seconds to transmit.

4.2.3.2 NAVIGATION MESSAGE CONTENT

The I/NAV message structures for E5b (1207.14 MHz) and for E1 (1575.42 MHz) frequency bands use the same page layout since the service provided on these frequencies is a dual frequency service. Only page sequencing is different; pages are swapped between both components in order to allow a fast reception of data by a dual frequency receiver. Nevertheless, the frame is designed to allow receivers to work with a single frequency as well [26]. The I/NAV type of navigation message is intended for the Safety-of-Life (SoL) service. There are two types of I/NAV pages [26]:

- Nominal page, which has a duration of 2 seconds transmitted sequentially in time in two parts (1 second each) in both E5 and E1 frequency bands. The first part of a page is denoted ‘even’, the other one is denoted ‘odd’;
- Alert page, which has a duration of 1 second transmitted in two parts (1 second each) at the same epoch over the E5b and E1 frequency band. The first part of a page is denoted ‘even’, the other one is denoted ‘odd’. This transmission is repeated at the next epoch (with the frequency bands of the two parts switched).

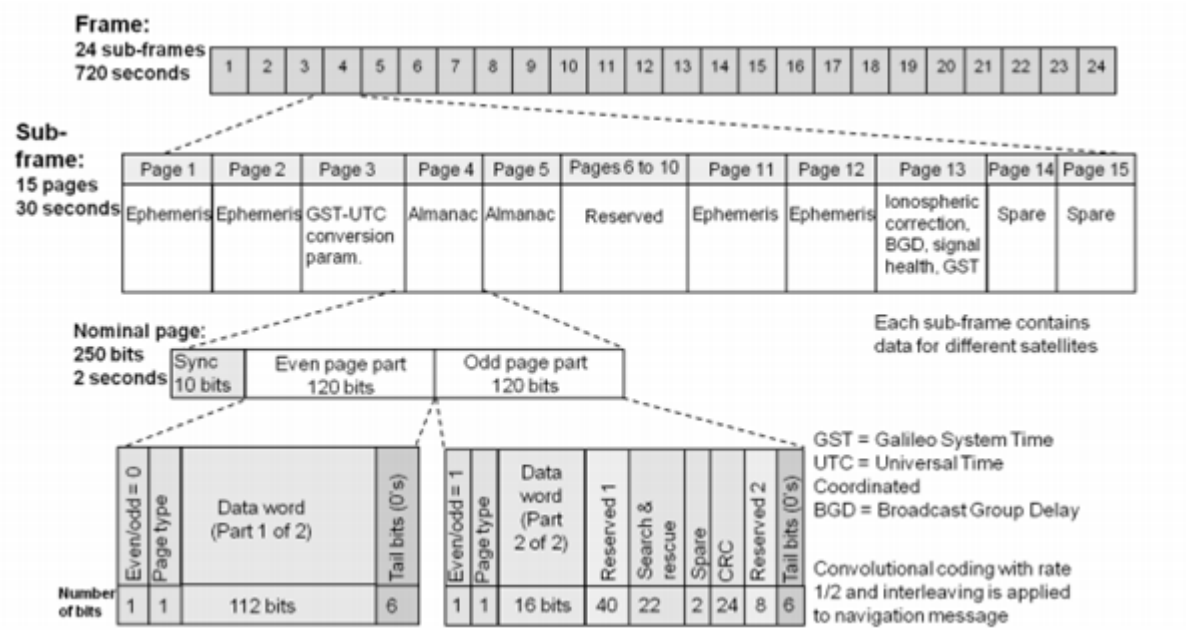

Figure 4. 3 Galileo E1 open service navigation message structure [18]

Each I/NAV page is the same for both types. It contains the synchronization pattern (0101100000) which is not encoded, an I/NAV page part of 114 bits, and tail bits composed of 6 zero-bits. These enable the completion of the FEC decoding of each page’s information content in the user receiver [26].

The I/NAV navigation message is transmitted at a rate of 125 bps and the I/NAV nominal frame contains sub-frames with almanac data.

4.4 BeiDou / Compass

Compass system (also known as BeiDou-2) is a Chinese project of which aim is to develop an independent satellite navigation system. The current system BeiDou-1 (made up of 4 satellites) is experimental and has limited coverage and applications. However, with the new Compass system, China plans to develop a truly global satellite navigation system consisting of 35 satellites [27].

4.4.1 System Overview

The system consists of three segments: the space segment, the control segment, and the user segment.

Space Segment

The new system will be a constellation of 35 satellites, which will include 5 geostationary orbit (GEO) satellites and 30 medium Earth orbit (MEO) satellites that will offer a complete coverage of the globe. Compass will offer 10 services. Five free, open services and five restricted services requiring authorization. These services will use eight different carrier frequencies.

Control Segment

Ground Control Segment consists of several Master Control Stations (MCS) and Upload Stations (US) and a network of globally distributed Monitor Stations (MS). The main tasks of the MCS are to collect observational data from each MS, to process data, to generate satellite navigation messages and wide area differential data and integrity information, to perform mission planning and scheduling, and to conduct system operation and control. The main tasks of the US include completing the upload of satellite navigation messages and wide area differential data and integrity information as well as controlling and managing the payload. The tasks of the MS include continuous tracking and monitoring of navigation satellites, receiving navigation signals, and sending observational data to the MCS for satellites orbit determination and time synchronization [28].

User Segment

The user segment includes various user terminals and terminals compatible with other navigation satellite systems.

4.4.2 COMPASS SIGNAL OVERVIEW

The Compass navigation signals are based on the code division multiple access (CDMA) technique. They use the binary phase shift keying (BPSK) modulation. BPSK (n) defines a BPSK modulation with a chip rate of n × 1.023 MHz.

The frequencies for Compass are allocated in four bands [29]:

- E1 = 1589.74 MHz; (4.10)
- E2 = 1561.10 MHz; (4.11)
- E5b = 1207.14 MHz; (4.12)
- E6 = 1268.52 MHz. (4.13)

The Compass signals may interfere and degrade the performance of Galileo, because Compass overlays the Galileo signals in the E2, E5b, and E6 bands [29].

4.4.3 NAVIGATION MESSAGE STRUCTURE

The Compass navigation message structure is similar to the structure of the GPS navigation message. There are two types of Compass navigation message: one is broadcast by MEO satellites (D1), the other one by GEO satellites (D2) [18].

4.4.3.1 D1 NAVIGATION MESSAGE FORMAT AND CONTENT

The D1 navigation message consists of a super-frame containing 24 frames (36,000 bits of data). Each frame includes 5 sub-frames, each sub-frame has 10 words. The transmit time of one message is 12 minutes.

- Sub-frames 1–3 are used to transmit information on time, clock correction data, health status, ephemeris, and ionosphere model parameters.
- Sub-frames 4–5 are used to transmit almanac for all satellites and information on the time offsets from other GNSS systems.

The first word in each sub-frame contains a preamble, sub-frame ID, week time data, and parity bits. The remaining words contain 22 bits of data followed by 8 parity check bits [18].

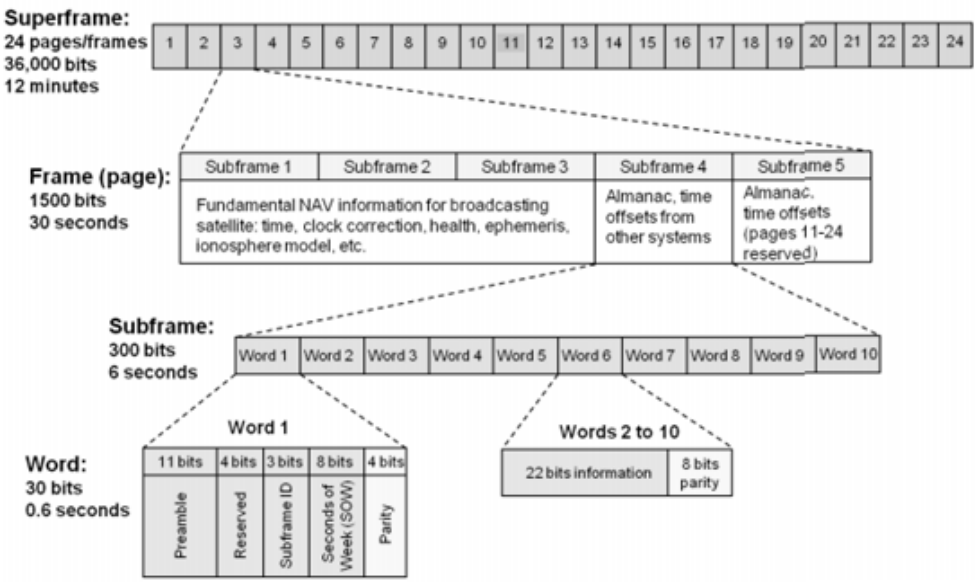

Figure 4. 4 Compass D1 navigation message structure transmitted at MEO [18]

4.4.3.2 D2 NAVIGATION MESSAGE FORMAT AND CONTENT

The D2 navigation message consists of a super-frame containing 120 frames (180,000 bits of data). The structure of the frames, sub-frames, and words is similar to D1. The transmit time of one message is 6 minutes.

- Sub-frame 1 contains basic navigation information.
- Sub-frames 2–4 contain system integrity and differential correction information.
- Sub-frame 5 contains the almanac, ionospheric model data, and time offsets from other GNSS systems [18].

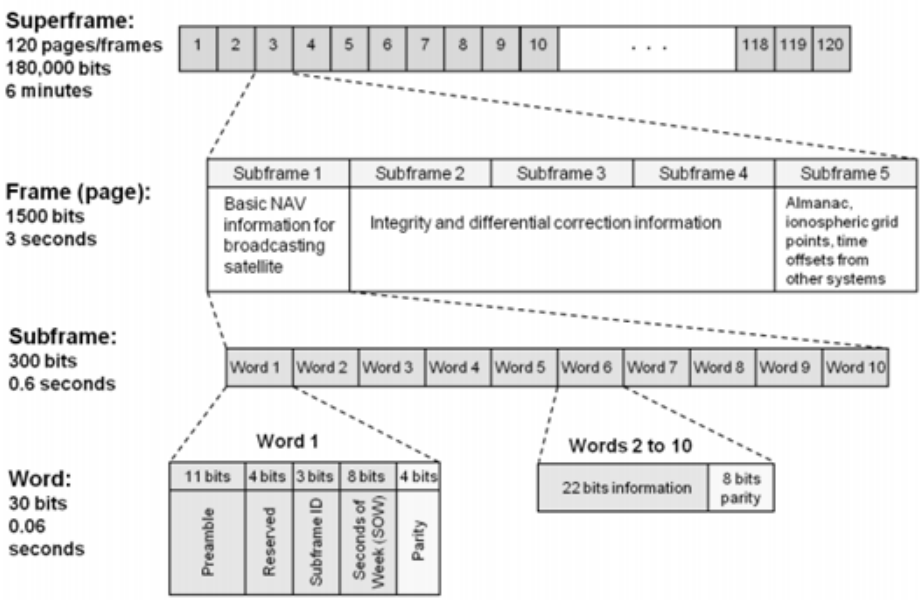

Figure 4. 5 Compass D2 navigation message structure transmitted at GEO [18]

5 GNSS AUGMENTATION SYSTEMS

Navigation based on the reception of signals from the GNSS satellites does not always provide adequate performance required for safety-critical applications such as sea-based or land-based automated aircraft navigation, landing systems, or navigation in environments with a high level of integrity.

Accuracy, integrity, and availability of global satellite navigation systems can be improved by the use of augmentation systems:

- Aircraft-Based Augmentation System (ABAS) – used to improve aircraft position;
- Space-Based Augmentation System (SBAS);
- Ground-Based Augmentation System (GBAS).

5.1 AIRCRAFT BASED AUGMENTATION SYSTEM (ABAS)

The most common ABAS technique is called receiver autonomous integrity monitoring (RAIM). RAIM requires redundant satellite range measurements to detect faulty signals and to alert the pilot. Its availability depends on the type of operation.

Another ABAS technique involves integration of GNSS with other airborne sensors such as inertial navigation systems.

An alternative to inertial navigation systems for oceanic and remote airspace operations is so called fault detection and exclusion (FDE) technique which is used to ensure that there will be enough satellites in view to support the planned flight [30].

5.2 SPACE BASED AUGMENTATION SYSTEM (SBAS)

The SBAS were primarily designed to improve core GNSS systems for aircraft navigation by providing ranging, integrity and correction information via geostationary satellites [30], [31].

The concept is based on:

- ground reference stations that monitor satellite signals;
- master stations that collect and process reference station data and generate SBAS messages;
- uplink stations that transmit differential corrections and integrity messages to geostationary satellites;
- transponders on these satellites that broadcast the SBAS messages.

The fully operational SBAS systems are:

- EGNOS (European Geostationary Navigation Overlay Service) in Europe;
- WAAS (Wide Area Augmentation System) in the USA;
- MSAS (Multi-functional Satellite Augmentation System) in Japan;
- GAGAN (GPS Aided Geo Augmented Navigation) in India.

The SBAS currently being developed are:

- SDCM (System of Differential Correction and Monitoring) in Russia;
- SNAS (Satellite Navigation Augmentation System) in China.

Future SBAS systems are under study in:

- South/Central America and the Caribbean - SACCSA (Solución de Aumentación para el Caribe, Centro y Sudamérica);
- Africa - AFI (Africa-Indian Ocean) region;
- Malaysia.

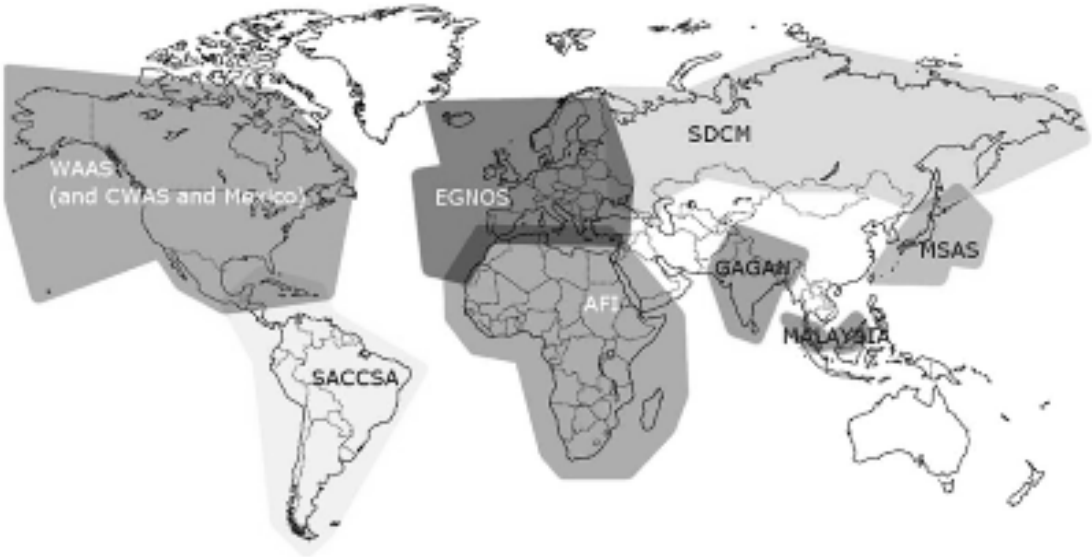

Figure 5. 1 SBAS in the world (source Pildo Labs)

5.2.1 EGNOS

The European Geostationary Navigation Overlay Service (EGNOS) is a joint project of the European Space Agency (ESA), the European Commission, and Eurocontrol, the European Organisation for the Safety of Air Navigation. Europe's first satellite-based system has augmented the GPS navigation system since 1st October 2009 and has made it suitable for safety critical applications [32].

The system consists of [33], [34]:

- a group of ground stations spread over Europe:
    - 39 RIMS (Ranging and Integrity Monitoring Stations) which are responsible for signal quality monitoring, satellite pseudorange measurements on GPS and SBAS geostationary satellites signals, Viterbi decoding, data demodulation, message formatting and transmission to MCC centres;
    - 4 MCC (Master Control Centres) which are responsible for a single set of integrity data generation and Wide Area Differential (WAD) GPS corrections for Europe;
    - 6 NLES (Navigation Land Earth Stations) which are responsible for reception of correction messages and uploading data back to the geostationary satellites;
- three geostationary satellites (two Inmarsat III satellites and one Artemis satellite);
- the user segment.

EGNOS offers three types of services:

- Open Service (OS) – data broadcasted through geostationary satellites, intended for market applications;
- Commercial Data Distribution Service (CDDS) – data broadcasted through the Internet, intended for commercial and professional users requiring enhanced performance;
- Safety of Life Service (SoL) – data broadcasted through geostationary satellites, intended for aviation.

5.2 GROUND BASED AUGMENTATION SYSTEM (GBAS)

The GBAS is a civil aviation safety critical system that provides a precision approach service (deviation guidance for final approach segments) and a positioning service (horizontal position information to support two-dimensional RNAV operations in terminal areas). A ground station at the airport broadcasts locally relevant corrections along with integrity parameters and approach data to aircrafts in the terminal area in the 108 – 117.975 MHz band [30].

Two main GBAS systems are the differential GPS (dGPS) and the Local Area Augmentation System (LAAS).

5.2.2 DIFFERENTIAL GPS (DGPS)

The dGPS improves accuracy and integrity of the GPS navigation system. Reference receivers of the dGPS are located at known positions. Ground-based reference station estimates an error between measured satellite pseudoranges and internally computed pseudoranges and transmits correction messages for each satellite in the view [35].

There are three main types of dGPS:

- Local Area dGPS;
- Wide Area dGPS;
- Carrier-Phase dGPS.

Differential corrections considerably improve accuracy for all users, regardless of whether selective availability (SA) is activated or not [35].

6 REFERENCE SYSTEMS IN GNSS

GNSS systems use a common reference frame (X, Y, Z) and an internal reference time scale for their positioning and timing solution [36].

6.1 COORDINATE SYSTEMS

The coordinate system used by the Global Positioning System (GPS) is the US Department of Defence standard called World Geodetic System 1984 (WGS84). The WGS84 coordinate system is a right-handed, Earth-fixed orthogonal coordinate system. It is based on a consistent set of constants and model parameters that describe the Earth's size, shape, and gravity and geomagnetic fields following the criteria outlined in the International Earth Rotation Service (IERS) Technical Note 21 [37], [38], [9].

The origin and axes are defined as follows [38]:

- Origin = the Earth's centre of mass;
- Z-axis = the direction of the IERS Reference Pole (IRP) which corresponds to the direction of the BIH Conventional Terrestrial Pole (CTP) (epoch 1984.0) with an uncertainty of 0.005";
- X-axis = intersection of the IERS Reference Meridian (IRM) and the plane passing through the origin and normal to the Z-axis. The IRM is coincident with the BIH Zero Meridian (epoch 1984.0) with an uncertainty of 0.005";
- Y-axis = completes a right-handed, Earth-Centred Earth-Fixed (ECEF) orthogonal coordinate system.

The WGS84 coordinate system origin also serves as the geometric centre of the WGS84 Ellipsoid. Likewise, the Z-axis serves as the rotational axis of this ellipsoid of revolution. It is compatible with the International Terrestrial Reference System (ITRS) [38].

The coordinate system used by GLONASS is the Parameters of the Earth 1990 System (PZ90). The PZ90 is an Earth-Centred Earth-Fixed (ECEF) coordinate system similar to the World Geodetic System 1984 (WGS84), but it slightly differs in setting parameters (transformation parameters are estimated between WGS84 and PZ90) [39].

The coordinate system used by Galileo is aligned to the Galileo Terrestrial Reference Frame (GTRF). Realisation and maintenance of the GTRF is the main function of the Galileo Geodetic Service Provider (GGSP). The GTRF is fully compatible with the latest International Terrestrial Reference Frame (ITRF) within a precision level of 3 cm (2 sigma) [40].

The connection to the ITRF is realized and validated by the International GNSS Service (IGS) stations. The current GTRF network solutions are based on GPS observations for the prototype implementation, with the intention to include Galileo observations as soon as the system reaches its operational stage [41].

The coordinate system used by Compass is the China Geodetic Coordinate System 2000 (CGCS 2000) realized by China Terrestrial Reference Frame 2000 (CTRF2000) which is referred to ITRF97 (epoch 2000.0). The system follows the criteria described by the IERS Technical Note No. 21. The reference ellipsoid used is the GRS1980 ellipsoid; the coordinate references of the Compass system and the GPS system are consistent [42].

6.2 TIME SCALES

GNSS systems rely on precise time. They use a clock ensemble for internal system synchronization, necessary to produce their positioning and timing solution [36].

GNSS system times are supposed to follow the recommendations of the International Telecommunication Union (ITU) and the General Conference on Weights and Measures (Conférence Générale des Poids et Mesures, CGPM), and to conform as closely as possible to the Coordinated Universal Time (UTC), including its leap seconds, otherwise they would gradually diverge.

UTC is a time scale for time dissemination. It is derived from the uniform atomic time scale International Atomic Time (TAI) by applying a correction of an integral number of seconds. UTC and TAI are maintained by the International Bureau of Weights and Measures (BIPM) and published on a monthly basis through the BIPM Circular T. From time to time, a leap second is added to the UTC whenever the International Earth Rotation and Reference Systems Service (IERS) recommends that an adjustment is necessary based on astronomical observations of the Earth's rotation. Local realizations of UTC (named UTC(k)) allow participating laboratories to monitor the steering of their clocks at shorter intervals than monthly.

TAI is a time scale defined in a geocentric reference frame with the SI second as realized on the rotating geoid as the scale unit. It is not used for time dissemination. In 2015, the difference between the continuous TAI and UTC amounts to 36 s [43].

Most GNSS systems do not apply leap seconds to their system times because of the difficulties associated with them; they adopt different strategies instead. In practice, only GLONASS system time actually follows UTC strictly including its leap seconds.

Various GNSS system times and their relations to the Coordinated Universal Time (UTC) and the International Atomic Time (TAI) are described below [44]:

GPS time: steered to UTC(USNO) modulo 1s (a continuous time scale without leap seconds)

- 19 s behind TAI
- 15 s ahead of UTC
- tolerance is 1 μs

GLONASS time: steered to UTC(SU) with leap seconds (not a continuous time)

- 34 s behind TAI
- equal to UTC
- tolerance is 1 ms

Galileo time: steered to a set of EU UTC(k), using GPS time seconds, GGTO (a continuous time scale without leap seconds)

- 19 s behind TAI
- 15 s ahead of UTC
- tolerance is 50 ns

BeiDou time: is linked to the Chinese UTC(k), which is consistent to UTC (a continuous time scale without leap seconds)

- 33 s behind TAI
- 1 s ahead of UTC
- tolerance is 100 ns

Satellite augmentation systems (such as WAAS, EGNOS, QZSS, etc.) use the GPS time.

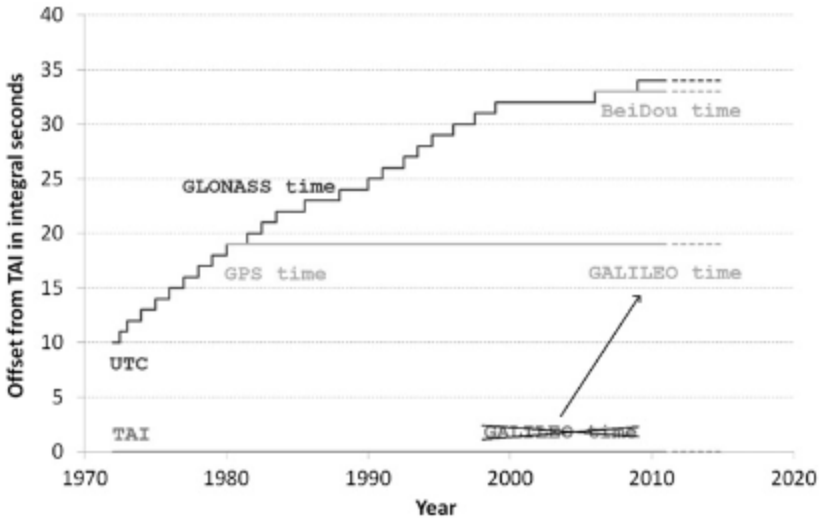

Figure 6. 1 Relationship between different time scales [44]

Receiver Computation of UTC

UTC time can be computed from a GPS signal as follows [9]:

$$UTC = t_{rcv} + t_u + t_n \,, \qquad (6.\ 1)$$

where t_{rcv} is the receiver clock time, t_u is the time bias from the GPS system time, t_n is the number of leap seconds between GPS system time and the UTC time.

As mentioned in [9], the above computation returns a value of UTC within 200 ns (95%) of the true UTC for PPS users, and 340 ns (95%) for SPS users.

7 CHARACTERISTIC OF ELECTROMAGNETIC WAVES

In order to understand the multipath effects, it is necessary to understand electromagnetic wave properties and the changes the GNSS signal goes through on the path from a satellite to a receiver.

7.1 PROPERTIES

Electromagnetic waves consist of electric and magnetic fields. These electric and magnetic fields, and especially how they affect each other in time, are described in Maxwell's four equations [45], [46] (Maxwell's own part is just the last term of the last equation – so called displacement current $\frac{\partial \vec{\mathbf{D}}}{\partial \mathrm{t}}$ – but it has dramatic importance in predicting the propagation of electromagnetic waves):

Gauss' law is the first of Maxwell's equations which describes how the electric field behaves around electric charges.

From the microscopic perspective:

$$\nabla \cdot \vec{\mathbf{E}} = \frac{\rho}{\epsilon_0}, \tag{7. 1}$$

where $\nabla \cdot$ is the divergence operator, $\vec{\mathbf{E}}$ is the electric field intensity [volt/m], ρ is the volume charge density [coulomb/m^3] and ϵ_0 is the vacuum permittivity.

$$\epsilon_0 = 8.854 \times 10^{-12} \text{ [farad/m]} \tag{7. 2}$$

From the macroscopic perspective:

$$\nabla \cdot \vec{\mathbf{D}} = \rho_f, \tag{7. 3}$$

where $\vec{\mathbf{D}}$ is the electric flux density (or the electric displacement) [coulomb/m^2] and ρ_f is the free charge density [coulomb/m^3].

Gauss' Magnetism law is the second of Maxwell's equations. It states that the magnetic flux through a closed surface is zero and that there are no magnetic monopole charges.

The microscopic and macroscopic equations are the same:

$$\nabla \cdot \vec{\mathbf{B}} = 0, \tag{7. 4}$$

where $\vec{\mathbf{B}}$ is the magnetic flux density (or the magnetic induction) [weber/m^2].

Faraday's law describes how the magnetic field induces the electric field in time.

The microscopic and macroscopic equations are the same:

$$\nabla \times \vec{\mathbf{E}} = -\frac{\partial \vec{\mathbf{B}}}{\partial \mathrm{t}}, \tag{7. 5}$$

where $\vec{\mathbf{E}}$ is the electric field intensity [volt/m] and $\vec{\mathbf{B}}$ is the magnetic flux density (or the magnetic induction) [weber/m^2].

Ampere's law + Maxwell's displacement current describe how electrical current and varying electric flux can induce a magnetic field.

From the microscopic perspective:

$$\nabla \times \vec{\mathbf{B}} = \mu_0 \vec{\mathbf{J}} \times \mu_0 \epsilon_0 \frac{\partial \vec{\mathbf{E}}}{\partial \mathrm{t}}, \tag{7. 6}$$

where $\vec{\mathbf{B}}$ is the magnetic flux density (or the magnetic induction) [weber/m^2], $\vec{\mathbf{J}}$ is the electric current density (charge flux) [ampere/m^2], ϵ_0 is the vacuum permittivity, $\vec{\mathbf{E}}$ is the electric field intensity [volt/m] and μ_0 is the vacuum permeability.

$$\mu_0 = 4\pi \times 10^{-7} \text{ [henry/m]} \tag{7. 7}$$

From the macroscopic perspective:

$$\nabla \times \vec{\mathbf{H}} = \vec{\mathbf{J_f}} + \frac{\partial \vec{\mathbf{D}}}{\partial \mathrm{t}}, \tag{7. 8}$$

where $\vec{\mathbf{H}}$ is the magnetic field intensity [ampere/m], $\vec{\mathbf{J_f}}$ is the free current density [ampere/m^2] and $\vec{\mathbf{D}}$ is the electric flux density (or the electric displacement) [coulomb/m^2].

7.2 POLARIZATION

Polarization is a phenomenon associated with transverse electromagnetic waves – i.e. plane waves where the electric and magnetic fields oscillate perpendicularly to each other and to the direction of propagation [47].

The direction of polarization of any electromagnetic wave is determined by the time-harmonic electric field intensity vector. There are three types of polarization: **linear, circular, and elliptic**.

Mathematical representation of a plane wave propagating in the direction x is [47], [48]:

$$E = E_0 \cos(kx - \omega t + \varphi_0), \quad (7.\ 9)$$

where E_0 is the amplitude, k is the propagation constant ($k = 2\pi/\lambda$), ω is the circular frequency ($\omega = kc = 2\pi c/\lambda$), φ_0 is the constant (or initial phase).

$$\varphi = (kx - \omega t + \varphi_0), \quad (7.\ 10)$$

where φ is the phase of the plane wave.

The electric field vector $\vec{E}$ may be decomposed into the parallel E_l and perpendicular E_r components as:

$$\vec{E} = E_l\vec{l} + E_r\vec{r}. \quad (7.\ 11)$$

Then equation (7. 11) can be expressed as:

$$E_l = E_{l0} \cos(kx - \omega t + \varphi_{l0}), \quad (7.\ 12)$$

$$E_r = E_{r0} \cos(kx - \omega t + \varphi_{r0}), \quad (7.\ 13)$$

we have

$$E_l/E_{l0} = \cos(v)\cos(\varphi_{l0}) - \sin(v)\sin(\varphi_{l0}), \quad (7.\ 14)$$

$$E_l/E_{r0} = \cos(v)\cos(\varphi_{r0}) - \sin(v)\sin(\varphi_{r0}), \quad (7.\ 15)$$

where $v = kx - \omega t$.

Then we obtain

$$(E_l/E_{l0})^2 + (E_r/E_{r0})^2 - 2(E_l/E_{l0})(E_r/E_{r0})\cos(\Delta\varphi) = \sin^2(\Delta\varphi), \quad (7.\ 16)$$

where $\Delta\varphi = \varphi_{l0} - \varphi_{r0}$ is the phase shift and equation (7. 16) defines an **ellipse** (or an elliptically polarized wave).

When $\Delta\varphi = n\pi$ $(n = 0, \pm1, \pm2, \ldots)$, $\sin(\Delta\varphi) = 0$ and $\cos(\Delta\varphi) = \pm 1$ and the equation below defines a **straight line** (or linearly polarized wave):

$$\left(\frac{E_l}{E_{l0}} \pm \frac{E_r}{E_{r0}}\right)^2 = 0 \quad (7.\ 17)$$

When $\Delta\,\varphi = n\,\pi/2$ $(n = \pm1, \pm3, \ldots)$ and $E_{l0} = E_{r0} = E_0$, then $\sin(\Delta\,\varphi) = \pm1$ and $\cos(\Delta\,\varphi) = 0$,

$$E_l{}^2 + E_r{}^2 = E_0{}^2, \qquad (7.\ 18)$$

and equation (7. 18) defines a **circle** (or circularly polarized wave).

Circularly polarized electromagnetic wave consists of two perpendicular electromagnetic plane waves of equal amplitude and 90° difference in phase.

Polarized electromagnetic waves can be also formed from non-polarized electromagnetic waves by processes as reflection, refraction, and scattering. The electric field component of a non-polarized electromagnetic wave oscillates randomly in the plane perpendicular to the direction of the wave path.

7.3 PROPAGATION

Electromagnetic waves pass through the vacuum and through different layers of the Earth's atmosphere.

Electromagnetic waves do not propagate in straight lines (except in the vacuum where they travel at 3×10^{-8} m/s), they are bent as they pass through the Earth's atmosphere – this increases the travel time of the signal from a satellite to a receiver.

Propagation of electromagnetic signal in the urban area is mainly impacted by four phenomena, as illustrated in Figure 7. 3 [49], [50]:

Reflection: a wave enters a different medium; its parameters (i.e. speed, wavelength, and energy) may change at the boundary of the two media.

The **Law of Reflection** states that the angle of incidence *i* equals to the angle of reflection *r*, as in Figure 7. 1. Furthermore, the incident ray, the normal to the surface, and the reflected ray all lie in the same plane.

$$i = r. \qquad (7.\ 19)$$

Most waves experience some loss of the signal and a phase shift upon reflection.

Refraction: a wave enters a different medium; this is followed by the change of direction, speed of propagation, and energy at the boundary of the two media.

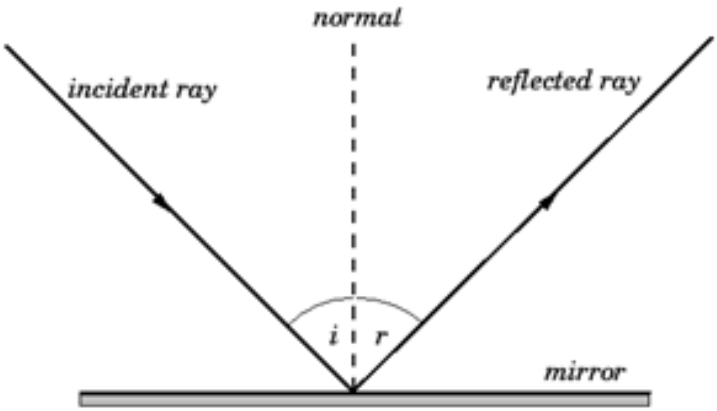

Figure 7. 1 Law of Reflection [50]

The **Snell's law / The Law of Refraction** is used to describe the relationship between the incident angle and the refracted angle:

$$n_1 \cdot \sin\theta_1 = n_2 \cdot \sin\theta_2 \tag{7. 20}$$

where n_1 is the refractive index in medium 1, n_2 is the refractive index in medium 2, $\theta_1$is the incident angle, $\theta_2$is the refracted angle, Figure 7. 2. This causes the direction of the signal to bend rather than change direction quickly.

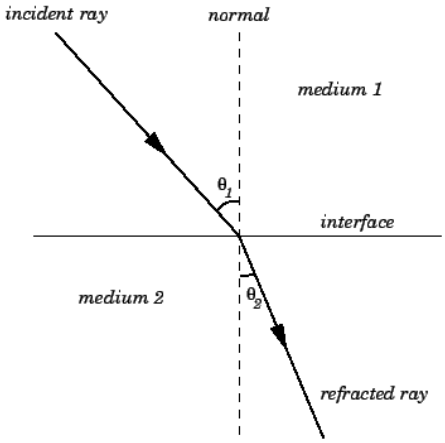

Figure 7. 2 Snell's law [50]

The permeability and permittivity in matter are larger than in vacuum $\mu > \mu_0$, and $\epsilon > \epsilon_0$ and determine the phase velocity v and the refractive index n:

$$v = \frac{1}{\sqrt{\mu\epsilon}} \tag{7. 21}$$

$$n = \frac{c}{v} = \frac{\sqrt{\mu\epsilon}}{\sqrt{\mu_0\epsilon_0}} \tag{7. 22}$$

Diffraction: bending of a wave as it travels past the edge of or around sharps corners (for more, look at Huygens' Principle of wave diffraction).

Scattering: a wave reflects at all angles (i.e. reflection that does not obey the Law of Reflection).

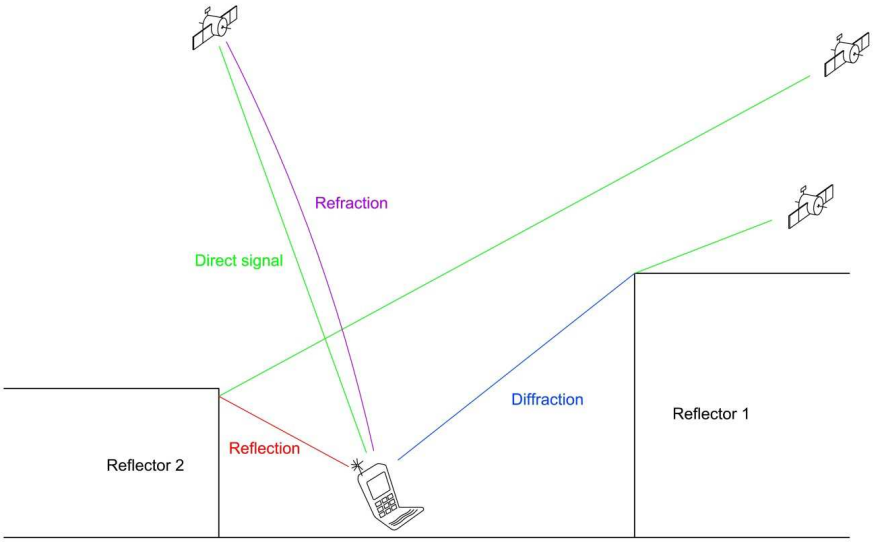

Figure 7. 3 GNSS signal propagation effects in urban environment

8 REPRESENTATION OF GNSS SIGNAL

Typically, an antenna receives the direct signal and one or more of its reflections from objects in the surroundings, including reflection from the ground.

Received signals may be classified into three main types:

- direct signals (LOS, line-of-sight) signals;
- indirect signals (NLOS, non-line-of sight) signals;
- blocked signals.

8.1 DIRECT SIGNAL

The general form of the direct line-of-sight (LOS) GNSS signal at the intermediate frequency (IF) may be written as [2]:

$$s_{LOS}(t) = A_0(t)G_d(t)D(t-\tau_0)x(t-\tau_0)\cos(2\pi(f_{IF}+f_D)t+\phi_d(t)), \qquad (8.\ 1)$$

where $A_0(t)$ is the amplitude of the signal-in-space, $G_d(t)$ is the antenna gain applied to the direct signal, $D(t)$ is the navigation data bit, $x(t)$ is a spread-spectrum (ranging) code, f_{IF} is the intermediate frequency (Hz), $f_d$is the Doppler shift (Hz), ϕ_d is the phase offset of the direct signal (rad), and τ_0 is the arrival time (delay) of the signal. It is assumed that the front-end bandwidth is wide enough to preserve the complete bandwidth of the signal. This signal is down converted to baseband by mixing it with a locally generated carrier modulated at the intermediate frequency plus a Doppler frequency estimate:

$$s_{Local}(t) = \cos\left(2\pi\left(f_{IF}+\hat{f}_D\right)t+\hat{\phi}_d(t)\right), \qquad (8.\ 2)$$

$$s(t) = s_{Local}(t)\cdot s_{LOS}(t), \qquad (8.\ 3)$$

where $\hat{f}_D$ and $\hat{\phi}_d(t)$ are initially estimated during acquisition and subsequently updated by the carrier tracking loop. To model multipath effects, one can simplify equation (8. 3) by assuming that the navigation data bits do not change, the signal in space amplitude A_0 is constant, and the Doppler frequency estimate error is negligible over the integration time.

The resulting signal is:

$$s(t) = A_0G_dx(t-\tau_0)\cos(\phi_d(t)). \qquad (8.\ 4)$$

It is a function of the signal amplitude, antenna gain, ranging code, and phase offset only.

At the satellite, a GNSS signal is well modelled [2]:

$$s(t) = \sqrt{2P_{tmt}}D(t)x(t)\,cos(2\pi f_L t + \theta_{tmt}). \quad (8.\ 5)$$

Neglecting the navigation message and assuming that the signal carries the C/A code only, the input signal at a certain epoch t can be simplified according to [51] as:

$$s_{LOS}(t) = \mathrm{A} \cdot \mathrm{C}(t - \tau_0) \cdot cos(\omega_0 t + \gamma_0). \quad (8.\ 6)$$

8.2 INDIRECT SIGNAL

Direct signal is normally the most wanted signal. Nevertheless, signals can also arrive at a receiver via a number of different paths that may occur between a transmitter and a receiver. These paths are results of reflections and diffractions from buildings, mountains, water, ground etc. They represent a dominant error source in precise positioning applications.

Reflected signal is a delayed and usually weaker version of the direct signal.

At the receiver, we find [2]:

$$r(t) = \sqrt{2P_{rcv}}D(t - \tau)x(t - \tau)\,cos(2\pi(f_L + f_D)t + \theta_{rcv}) + n(t). \quad (8.\ 7)$$

Where $\sqrt{2P}$ is an amplitude, $D(t)$ is the navigation data, $x(t)$ is a spread spectrum code, $\cos(2\pi f t + \theta)$ is the radio frequency carrier, $n(t)$ is the noise and $P_{tmt\ (transmitted)} >> P_{rcv\ (received)}$.

Neglecting the navigation message and assuming that the signal carries the C/A code only, the input signal at a certain epoch t can be simplified according to [51] as:

$$r(t) = s_{LOS}(t) + s_i(\mathrm{t}) \quad (8.\ 8)$$

$$= \mathrm{A} \cdot \mathrm{C}(t - \tau_0) \cdot cos(\omega_0 t + \gamma_0) + \sum_{i=0}^{n} \alpha_i \cdot \mathrm{A} \cdot \mathrm{C}(t - \tau_0 + \tau_i) \cdot cos(\omega_0 t + \gamma_0 + \gamma_i).$$

8.3 RELATIONSHIP BETWEEN DIRECT AND INDIRECT SIGNAL

Reflected signals represent a major source of error in satellite-based systems: They distort the signal modulation, they affect both code and carrier measurements, and hence significantly degrade the positioning accuracy. They also increase the time needed for receiver initialization.

Reflected signals take more time to reach the receiver than the direct signals. This path delay, or rather this difference between the length of the path taken by the reflected signal

and the direct path between a satellite and a receiver, causes an important pseudorange measurement error.

As per [2], typical multipath error in pseudorange measurements ranges from 1 m (in a fair environment) to over 5 m (in highly reflective environment) and the phase measurement error doesn't exceed a quarter cycle (if the reflected signal is of a smaller amplitude than the direct signal).

Reflected GNSS signals have a set of characteristics that are different from those of directly received signals. The most important are:

1) Polarization – GNSS signals are right-hand circularly polarized (RHCP). Once the signal is reflected, it changes its polarization to left-hand.

2) Carrier Phase, Doppler Shift – both changes after reflection; the impacts are larger when the path delay is short.

Consider a situation where an antenna receives two signals: a direct signal and a delayed reflected signal with phase shift $\Delta\phi$ and amplitude attenuation α [2]:

$$received\ signal = A\cos\phi + \alpha\, A\cos(\phi + \Delta\phi). \quad (8.\ 9)$$

The error in the carrier phase measurement due to the multipath is as:

$$\delta\phi = \arctan\left(\frac{\sin\Delta\phi}{\alpha^{-1} + cos\Delta\phi}\right). \quad (8.\ 10)$$

In the worst case $\delta\phi = 90°,\ \alpha > 1$.

3) Code phase – the resulting code tracking error depends on the path delay, phase difference, and the strengths of the direct and reflected signals as well as on the design of the receiver.

4) Correlation – reception of reflected signals causes distortion in the code correlation peak within the receiver. Therefore, the code phase of the direct signal, which is used to generate the pseudorange, cannot be determined precisely.

5) Signal Power – reflected signals can be weaker or stronger compared to the direct signals. High-sensitivity receivers can acquire much weaker signals; however, they can also receive significantly more reflected signals - more about this topic e.g. in [52].

GNSS signals are extremely weak when arriving at a user receiver – they even are below the noise level. It is the knowledge of the signal structure (spread code) that allows a receiver to recover the signal from noise and perform precise measurements.

The spread code allows a receiver to obtain the information on the signal delay by correlation with a replica of the satellite code (in other words, the distance to the satellite). If the signal is degraded by multipath propagation, the peak of the correlation function becomes less significant and the accuracy of the delay measurement is therefore reduced.

Future satellites may have higher signal power to make the service more robust.

System	Signal	Minimum power level (dBW)
GPS	L1 C/A	-158.5
	L2 C (satellite type II/IIA/IIR)	-164.5
	L2 C (satellite type IIR-M/IIF)	-160
	L5 I and Q	-157.9
GLONASS	L1 and L2 (all satellite types)	-161
Galileo	E1 (L1)	-157
	All other than E1 (L1) frequencies	-155

Table 8. 1 Minimum power levels of GNSS signals [53]

As an example, the minimum received signal power for L1 C/A can be computed as [9]:

The L1 C/A code signal is transmitted at a minimum level of 478.63 W (26.8 dBW) effective isotropic radiated power $EIRP.$ As the signal propagates, it losses power density due to spherical spreading. The loss is accounted by a quantity called the free-space loss factor $FSLF$ given by:

$$FSLF = (\frac{\lambda}{4\pi R})^2, \quad (8.\ 11)$$

where R is a distance from the transmitting antenna compared to a value normalized to unity at the distance $\lambda/4\pi$ meters from the antenna phase centre.

L1 C/A => $FSLF$ is about -184.4 dB. Total atmospheric loss factor $ALF,$ L1 C/A => ALF is about 0.5 dB.

Receiver antenna gain $RAG.$ The minimum received signal power for a typical GPS antenna is about 3.0 dB larger.

Polarization mismatch loss PML: L1 C/A => 3.4 dB.

Minimum received signal power for L1 C/A is:

$$EIRP - FSLF - ALF + RAG - PML = 26.8 - 184.4 - 0.5 + 3.0 - 3.4 = -158.5\ \text{dBW}. \quad (8.\ 12)$$

9 GNSS ANTENNAS AND RECEIVERS

9.1 BASIC ANTENNA CONCEPT

Antennas play a key role in receiver system design and with the modernization of existing GNSS systems becoming a larger factor for product designers and users too.

The antenna is the first element in the signal path before radio-frequency (RF) front end. To describe its performance, three main parameters have to be considered: frequency/bandwidth, gain pattern and polarization [13].

9.1.1 FREQUENCY/BANDWIDTH

The antenna induces a voltage from radio waves and accommodates the appropriate bandwidth of the desired signal - this is specified in two additional parameters:

Voltage Standing Wave Ratio (VSWR) – is typically 2.0:1, which equates to 90% power absorption across the bandwidth of desired frequencies. Impedance – generally all front end components use an impedance of 50Ω.

9.1.2 GAIN PATTERN

The antenna pattern describes the directivity of the antenna. The preferred antenna pattern for GNSS signals is hemispherical, design to receive signals from only positive elevation angles from all azimuth directions. Due to the multipath, low elevation angles signals are eliminated and signals only above 10° - 20° elevation are taken into account, decreasing the availability of satellite measurements.

The most popular GNSS GPS L1 antenna implementations are the patch and helix approaches but others also exists.

9.1.3 ANTENNA POLARIZATION

Polarization is one of the main characteristics of any antenna which occurs only with a transverse wave.

A GNSS signal is right-hand circularly polarized (RHCP). Therefore, most of the GNSS antennas are designed for right-hand circular polarization (RHCP) to match the polarization of the incoming GNSS signal and thus to achieve its best quality. In some limited cases, it is possible to use GNSS antennas with polarization diversity or linearly polarized (LP) antennas [13]. Changes in polarization cause degradation of quality of received signal.

One of the most difficult errors to mitigate for GNSS is multipath - most reflected signals have left-handed circular polarization (LHCP) or mixed polarization. An RHCP antenna can

quite effective supress the LHCP reflection and therefore minimize multipath reflection error. Naturally, a second reflection will cause the RHCP polarization again, but with the multiple reflections the signal power is reduced and the receiver does not consider such a signal to the computation of user position.

9.2 BASIC RECEIVER CONCEPT

The signal processing for satellite navigation system is based on a channelized structure. Before allocating a channel to a satellite, the receiver has to know which satellites are visible to the user. There are two common ways of finding the initially visible satellites [13]:

- *Warm start* – to compute which satellites should be visible, the receiver combines information in stored almanac data and the last position computed by the receiver. In the case the receiver has been moved far away since it was turned off, the receiver position cannot be trusted and the found satellites do not match the actual visible satellites. Another case is that the almanac data can be outdated. In either case, the receiver has to make a cold start.

- *Cold start* – the receiver doesn't use any stored information, it starts from scratch searching for satellites. This method is called acquisition and it is quite time consuming process, therefore a warm start is preferred if possible.

Standard receiver functions can be classified into three categories [54]:

- Radio – Frequency Front End
- IF Signal Processing
- Computation of Position

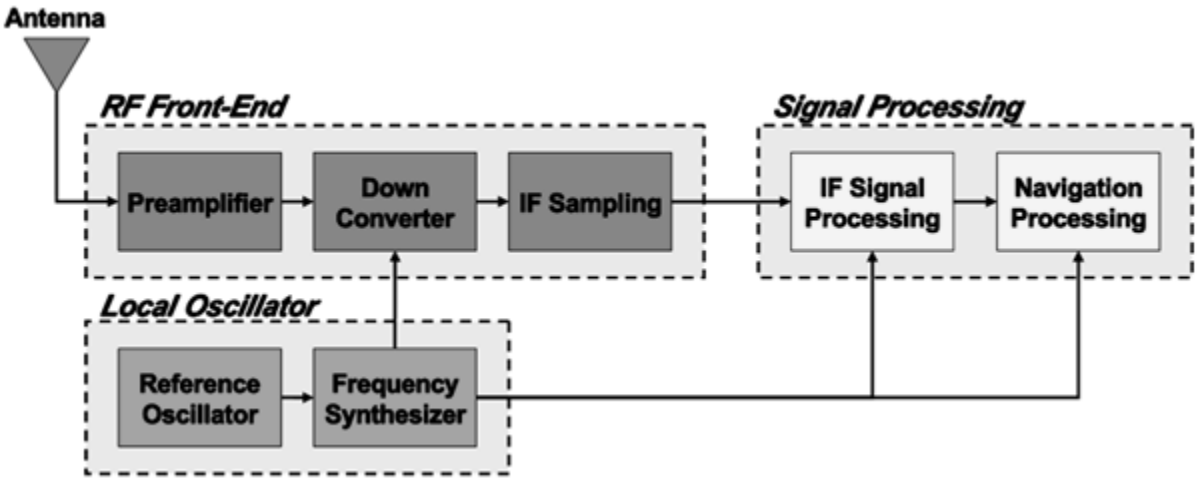

Figure 9. 1 Standard receiver functions [54]

9.2.1 RF FRONT END

The main objective of the RF front end is to convert RF carrier frequency (i.e. GPS L1 1575.42 MHz) to a lower intermediate frequency IF (typically in tens of MHz) so it is easier to work with. The IF signal is then sampled and processed in the signal processing part of the receiver [54].

9.2.2 SIGNAL PROCESSING

The primary purpose of GNSS signal processing is to generate a local signal that perfectly matches the incoming signal.

In general, signal processing for a given signal can be done in stages called: Acquisition, Tracking, Navigation Data Extraction, Pseudorange Computation and finally Computation of User Position.

9.2.2.1 ACQUISITION

Acquisition is the first step in processing the sampled IF signal. The main purpose of acquisition is to find all visible satellites and to determine coarse estimates of the following two parameters of the satellite signal:

Frequency – the frequency of the signal from a specific satellite can differ from its nominal value. It is caused by the motion of the satellite relative to the GNSS receiver, referred as to a Doppler frequency shift. For a stationary receiver the maximum Doppler frequency shift for the L1 frequency is ± 5kHz, for a dynamic receiver moving at a high speed it is ±10kHz [55]. The Doppler frequency shift affects both the acquisition and tracking of the signal.

Code Phase – the code phase indicate the point in the current data block where the C/A code begins. The satellites are differentiated by the 32 different PRN sequences. The code phase is the time alignment of the PRN code in the current block of data. It is necessary to know the code phase in order to generate a local PRN code that is perfectly aligned with the incoming code.

The received signal $s(t)$ is a combination of signals from all visible satellites [13]:

$$s(t) = s^1(t) + s^2(t) + s^3(t) + \cdots + s^n(t). \quad (9.\ 1)$$

When acquiring satellite *k*, the incoming signal *s(t)* is multiplied with the local generated C/A code corresponding to the satellite *k*. The cross correlation between C/A codes for different satellites causes signals from other satellites are nearly removed by this procedure.

PRN codes have high correlation only for zero lag. It means that the two signals have to be perfectly aligned in time to remove the incoming code.

After that, the signal is mixed with a locally generated carrier wave to remove the incoming carrier from the signal. To identify whether or not a satellite is visible, it is sufficient to search the frequency in steps of 500 Hz resulting in 41 different frequencies in case of a fast moving receiver (maximum change up to ±10kHz) and 21 in case of a static receiver (maximum change up to ±5kHz) [56].

The acquisition procedure works as a search procedure. Multiplication with the locally generated carrier signal generates the in-phase signal *I*, and with a 90° phase-shift the quadrature signal *Q*. The *I* and *Q* signals are integrated over 1ms (corresponding to the length of one C/A code), and squared and summed providing a numerical value.

For each of the different frequencies 1023 different code phases are tried:

$$1023\left(2\frac{10{,}000}{500}+1\right)=1023\times 41=41{,}943\ \text{combinations.} \qquad (9.\ 2)$$

Then a search for the maximum value is performed. If the maximum value exceeds a predefined threshold, the frequency and code phase are correct and can be passed on to the tracking process [57].

9.2.2.2 TRACKING

The main purpose of tracking is to refine the rough values of frequency and code phase, keep track, demodulate the navigation data and provide an estimate of the pseudorange. The tracking is done continuously to follow the changes in frequency as a function of time. If the track is lost, a new acquisition must be performed.

The tracking contains two parts [13]:

- *Code tracking* – implemented as a delay lock loop (DLL) where three local replicas (early, prompt and late) are generated and correlated with the incoming signal. The replicas are often separated by a half-chip length.

- *Carrier frequency / phase tracking* – done in two ways; either by tracking the frequency of the signal or by tracking the phase.

So to ideally track and demodulate the satellite signal, the tracking process has to generate two replicas, one for the carrier and one for the code. First the signal is multiplied with a carrier replica and then with a code replica. When the signals are properly tracked, the

C/A code and the carrier wave can be removed from the signal, only leaving the navigation data bits.

9.2.2.3 NAVIGATION DATA EXTRACTION

The output of tracking process gives the navigation message.

After reading about 30s of data, the beginning of a sub-frame must be determined in order to find the time when the data was transmitted from the satellite. After this procedure, the ephemeris data for the satellite must be decoded to use it later for the position computations.

9.2.2.4 PSEUDORANGE COMPUTATIONS

The last thing to do before making position computations is to compute pseudoranges. A pseudorange is the time the signal has travelled from the satellite to the receiver, multiplied by the speed of light. The time of arrival at the receiver is based on the beginning of the sub-frame.

Because the time of transmission from the satellite and the time of arrival at the receiver are different in the time scale, it is impossible to measure the true range between them – therefore we speak of pseudoranges rather than ranges.

Let the true geometrical range between satellite k and receiver i be denoted ρ_i^k [13]:

$$\rho_i^k = \sqrt{(X^k - X_i)^2 + (Y^k - Y_i)^2 + (Z^k - Z_i)^2}. \quad (9.\ 3)$$

Let c denote the speed of light, dt_i be the receiver clock offset, dt^k be the satellite clock offset, T_i^k be the tropospheric delay, I_i^k be the ionospheric delay and e_i^k be the observational error of the pseudorange. Then the basic equation for the pseudorange P_i^k is:

$$P_i^k = \rho_i^k + c(dt_i - dt^k) + T_i^k + I_i^k + e_i^k. \quad (9.\ 4)$$

Inserting equation (9. 3) into equation (9. 4) yields

$$P_i^k = \sqrt{(X^k - X_i)^2 + (Y^k - Y_i)^2 + (Z^k - Z_i)^2} + c(dt_i - dt^k) + T_i^k + I_i^k + e_i^k. \quad (9.\ 5)$$

Equation (9. 5) is nonlinear with respect to the receiver position(X_i, Y_i, Z_i).

9.2.2.5 COMPUTATION OF POSITION

The final task of the receiver is to compute a user position. The position is computed from pseudoranges and satellite positions (X^k, Y^k, Z^k) found from ephemerides data.

The most commonly used algorithm for position computations from pseudoranges is based on the method of least-squares [57]. This method is used when there are more observations than unknowns.

The position of the satellite (X^k, Y^k, Z^k) and satellite clock offset dt^k are found in the ephemerides, the tropospheric delay T_i^k and the ionospheric delay I_i^k are computed from different a priori models, the error e_i^k is minimized by using the least-squares method.

There are four unknowns in the equation (X, Y, Z and dt) and therefore to compute the position at least four pseudoranges are needed. Before using the last-squares method the equation (9. 5) has to be linearized.

Linearization

$$f(X,Y,Z) = \sqrt{(X^k - X)^2 + (Y^k - Y)^2 + (Z^k - Z)^2}. \quad (9.\ 6)$$

Linearization stars by finding an initial position for the receiver (X_0, Y_0, Z_0). This is often chosen as the center of the Earth $(0, 0, 0)$.

The approximate receiver coordinates are updated by increments ΔX, ΔY, ΔZ defined as:

$$X_1 = X_0 + \Delta X\ , \quad (9.\ 7)$$

$$Y_1 = Y_0 + \Delta Y\ , \quad (9.\ 8)$$

$$Z_1 = Z_0 + \Delta Z\ , \quad (9.\ 9)$$

$$f(X_1, Y_1, Z_1) = f(X_0 + \Delta X, Y_0 + \Delta Y, Z_0 + \Delta Z). \quad (9.\ 10)$$

The Taylor expansion of $f(X_0 + \Delta X, Y_0 + \Delta Y, Z_0 + \Delta Z)$ begins with terms:

$$f(X_1, Y_1, Z_1) = f(X_0, Y_0, Z_0) + \frac{\partial f(X_0,Y_0,Z_0)}{\partial X_0}\Delta X + \frac{\partial f(X_0,Y_0,Z_0)}{\partial Y_0}\Delta Y + \frac{\partial f(X_0,Y_0,Z_0)}{\partial Z_0}\Delta Z. \quad (9.\ 11)$$

The partial derivatives come from the square root f in (9. 6):

$$\frac{\partial f(X_0,Y_0,Z_0)}{\partial X_0} = -\frac{X^k - X_0}{\rho^k}\ , \quad (9.\ 12)$$

$$\frac{\partial f(X_0,Y_0,Z_0)}{\partial Y_0} = -\frac{Y^k - Y_0}{\rho^k}, \quad (9.\ 13)$$

$$\frac{\partial f(X_0,Y_0,Z_0)}{\partial Z_0} = -\frac{Z^k - Z_0}{\rho^k}. \quad (9.\ 14)$$

Let ρ_0^k be the range computed from the approximate receiver position:

$$\rho_0^k = \sqrt{(X^k - X_0)^2 + (Y^k - Y_0)^2 + (Z^k - Z_0)^2}. \quad (9.\ 15)$$

The four first order linearized observation equations become:

$$P^k = \rho_0^k - \frac{X^k - X_0}{\rho_0^k}\Delta X - \frac{Y^k - Y_0}{\rho_0^k}\Delta Y - \frac{Z^k - Z_0}{\rho_0^k}\Delta Z + c(dt - dt^k) + T^k + I^k + e^k. \quad (9.\ 16)$$

The least-squares method

A least-squares problem is given as a system $\mathbf{Ax} = \mathbf{b}$ with no exact solution. $\mathbf{A}$ has m rows and n columns, with $m > n$. There are more observations $\mathbf{b_1}, \ldots, \mathbf{b_m}$ than unknowns $\mathbf{x_1}, \ldots, \mathbf{x_m}$. The best choice $\hat{\boldsymbol{x}}$ minimizes the length of the error vector $\hat{\boldsymbol{e}} = \mathbf{b} - \mathbf{A}\hat{\boldsymbol{x}}$.

The least-square solution comes from the normal equations for the linearized problem:

Normal equations is:

$$\mathbf{A^T A x} = \mathbf{A^T b}\,, \quad (9.\ 17)$$

or

$$\mathbf{x} = (\mathbf{A^T A})^{-1}\mathbf{A^T b}. \quad (9.\ 18)$$

The covariance matrix for the parameters $\hat{\boldsymbol{x}}$ is:

$$\Sigma_{\hat{x}} = \hat{\sigma}_0^2 (A^T A)^{-1}\,, \quad (9.\ 19)$$

with

$$\hat{\sigma}_0^2 = \frac{\hat{e}^T \hat{e}}{m-n}\,. \quad (9.\ 20)$$

To reach $\mathbf{Ax} = \mathbf{b}$, the linear observation equation is rewritten in a vector formulation:

$$P^k = \rho_0^k + \left[-\frac{X^k - X_0}{\rho_0^k} \; -\frac{Y^k - Y_0}{\rho_0^k} \; -\frac{Z^k - Z_0}{\rho_0^k} \; 1\right] \begin{bmatrix} \Delta X \\ \Delta Y \\ \Delta Z \\ c\,dt \end{bmatrix} - c\,dt^k + T^k + I^k + e^k. \quad (9.\ 21)$$

We rearrange this in the usual formulation of a least-squares problem $\mathbf{Ax} = \mathbf{b}$

$$\left[-\frac{X^k-X_0}{\rho_0^k}\ -\frac{Y^k-Y_0}{\rho_0^k}\ -\frac{Z^k-Z_0}{\rho_0^k}\ 1\right]\begin{bmatrix}\Delta X\\ \Delta Y\\ \Delta Z\\ c\ dt\end{bmatrix}=P^k-\rho_0^k+c\ dt^k-T^k-I^k-e^k. \qquad (9.\ 22)$$

A unique least-square solution cannot be found until there are $m \geq 4$ equations. In our problem $b^k = P^k - \rho_0^k + c\ dt^k - T^k - I^k - e^k$, and the unknowns are the updates to X, Y, Z, dt:

$$\mathbf{Ax} = \begin{bmatrix} -\frac{X^1-X_0}{\rho_0^1} & -\frac{Y^1-Y_0}{\rho_0^1} & -\frac{Z^1-Z_0}{\rho_0^1} & 1 \\ -\frac{X^2-X_0}{\rho_0^2} & -\frac{Y^2-Y_0}{\rho_0^2} & -\frac{Z^2-Z_0}{\rho_0^2} & 1 \\ -\frac{X^3-X_0}{\rho_0^3} & -\frac{Y^3-Y_0}{\rho_0^3} & -\frac{Z^3-Z_0}{\rho_0^3} & 1 \\ & \vdots\ \vdots\ \vdots & & \\ -\frac{X^m-X_0}{\rho_0^m} & -\frac{Y^m-Y_0}{\rho_0^m} & -\frac{Z^m-Z_0}{\rho_0^m} & 1 \end{bmatrix}\begin{bmatrix}\Delta X_1\\ \Delta Y_1\\ \Delta Z_1\\ c\ dt_1\end{bmatrix} = \mathbf{b} - \mathbf{e}\,. \qquad (9.\ 23)$$

The solution ΔX_1, ΔY_1, ΔZ_1 is added to approximate receiver position to get the next approximate position:

$$X_1 = X_0 + \Delta X_1\,, \qquad (9.\ 24)$$

$$Y_1 = Y_0 + \Delta Y_1\,, \qquad (9.\ 25)$$

$$Z_1 = Z_0 + \Delta Z_1\,. \qquad (9.\ 26)$$

These iterations continue until the solution ΔX_1, ΔY_1, ΔZ_1 is at meter level. Often three iterations are sufficient to obtain that goal.

9.2.3 LOCAL OSCILLATOR

The reference oscillator is a device that produces a periodic output and is commonly based on quartz crystal local oscillators (LO) or atomic frequency standards.

The frequency synthesizer uses the output of the reference oscillator to generate a particular frequency (in this case a sinusoid) [58].

10 GLOBAL NAVIGATION SATELLITE SYSTEM ERROR ANALYSIS

10.1 OVERVIEW OF THE SOURCES OF ERROR

The accuracy with which a user receiver determines its position is primarily affected by two things:

1. the satellite geometry (which causes geometric dilution)
2. ranging error sources

The accuracy can be then expressed as the product of a geometry element and a ranging error element [9]:

$$(\text{error in GNSS solution}) = (\text{geometry dilution element}) \text{ x } (\text{ranging error element}). \quad (10.\ 1)$$

10.2 GEOMETRIC DILUTION OF PRECISION (GDOP)

The geometry element is termed the dilution of precision (DOP) and expresses the positional differences between the receiver and the satellites.

It is a powerful tool for GNSS – based on it, receivers use some algorithms to select the best set of satellites in the view to acquire and track. Typical dilution factors range from 1.5 to 8. The results can be affected by geometry when the factor reaches 5 and more [58].

Example Calculations

As in [58], the well – known GDOP equation can be written:

$$cov(position) = \sigma_R^2 \cdot [\boldsymbol{G}^T \boldsymbol{G}]^{-1}, \quad (10.\ 2)$$

where $[\boldsymbol{G}^T \boldsymbol{G}]^{-1}$ is the GDOP matrix (the matrix of multipliers of ranging variance to get position variance) and σ_R^2 (m^2) ranging variance.

If the position coordinates are the ordered right-hand set, then the square root of the ordered diagonal terms from the upper left are: east DOP, north DOP, vertical DOP, and time DOP.

$$cov(position) =$$

$$\sigma_R^2 \cdot \begin{bmatrix} (east\ DOP)^2 & cov\ term & cov\ term & cov\ term \\ cov\ term & (north\ DOP)^2 & cov\ term & cov\ term \\ cov\ term & cov\ term & (vertical\ DOP)^2 & cov\ term \\ cov\ term & cov\ term & cov\ term & (time\ DOP)^2 \end{bmatrix}. \quad (10.\ 3)$$

Let's define satellite direction as azimuth A – measured 360° clockwise from north, and elevation E – measured up from local horizontal (0°-90°). Then the $\mathbf{G}$ matrix becomes:

$$\mathbf{G} = \begin{bmatrix} (cos(E_1) * sin(A_1)) & (cos(E_1) * cos(A_1)) & sin(E_1) & 1 \\ (cos(E_2) * sin(A_2)) & (cos(E_2) * cos(A_2)) & sin(E_2) & 1 \\ (cos(E_3) * sin(A_3)) & (cos(E_3) * cos(A_3)) & sin(E_3) & 1 \\ (cos(E_4) * sin(A_4)) & (cos(E_4) * cos(A_4)) & sin(E_4) & 1 \end{bmatrix}. \quad (10.\ 3)$$

As in [58], the best accuracy is found with three satellites equally spaced on the horizon, at minimum elevation angle, and one satellite directly overhead, see Table 10. 1.

	satellite 1	satellite 2	satellite 3	satellite 4
Elevation – *E* (°)	5	5	5	90
Azimuth – *A* (°)	0	120	240	0

Table 10. 1 Satellite location [58]

For 5° minimum satellite elevation, the $\mathbf{G}$ and $\mathbf{G^{-1}}$ matrix become:

$$\mathbf{G} = \begin{bmatrix} 0.000 & 0.996 & 0.087 & 1.000 \\ 0.863 & -0.498 & 0.087 & 1.000 \\ -0.863 & -0.498 & 0.087 & 1.000 \\ 0.000 & 0.000 & 1.000 & 1.000 \end{bmatrix}, \quad (10.\ 4)$$

$$\mathbf{G}^{-1} = \begin{bmatrix} 0.000 & 0.580 & -0.580 & 0.000 \\ 0.670 & -0.335 & -0.335 & 0.000 \\ -0.365 & -0.365 & -0.365 & 1.095 \\ 0.365 & 0.365 & 0.365 & -0.095 \end{bmatrix}. \quad (10.\ 5)$$

Note that the last row gives the time solution (or bias in the local clock). The GDOP matrix for this example is shown as:

$$(\boldsymbol{G^T G})^{-1} = \begin{bmatrix} 0.672 & 0.000 & 0.000 & 0.000 \\ 0.000 & 0.672 & 0.000 & 0.000 \\ 0.000 & 0.000 & 1.600 & -0.505 \\ 0.000 & 0.000 & -0.505 & 0.409 \end{bmatrix}. \quad (10.\ 6)$$

For a greater number of satellites, $\mathbf{G}^{-1}$ is replaced with $(\mathbf{G^T G})^{-1}$. The results of the GDOP matrix above are:

HDOP (horizontal DOP) = 1.16, VDOP (vertical DOP) = 1.26, PDOP (position DOP) = 1.72, TDOP (time DOP) = 0.64, GDOP = 1.83.

With all 24 satellites available, PDOP becomes higher (up to 6 or 7) [58].

10.3 RANGING ERROR SOURCES

The range error element is referred to as the user equivalent range error (UERE) and expresses the total sum of the contributions from each of the error sources associated with the satellite (i.e. typical UERE for a single frequency L1 receiver is about 6 m [2]).

The main error sources can be grouped into the six following classes [58]:

- Ephemeris data errors
- Satellite clock errors
- Ionosphere errors
- Troposphere errors
- Multipath errors
- Receiver errors

10.3.1 EPHEMERIS DATA ERRORS

Ephemeris errors ensue when the navigation message does not transmit the correct satellite location. Predicted satellite ephemerides are included as a part of the 50 bps 1,500-bit navigation message that modulates the transmitted signal. The master control station of the control segment uploads the ephemeris data to each satellite that then transmits the data to users via the navigation message. Ground receivers then use the prediction for real time estimates of satellite coordinates and clock corrections. Data used for the predictions are acquired from receivers situated at precisely known locations. Small errors in the ephemeris data cause errors in the computed position of the satellite - typically resulting in range errors less than 1m [7].

10.3.2 SATELLITE CLOCK ERRORS

Although the atomic clocks in the satellites are highly accurate, errors can be large enough to require correction. The clocks are allowed some degree of relative drift that is estimated by ground station observations and is used to generate clock correction data in the navigation message. After the correction has been applied, the remaining error is typically less than 1 m in range [7].

10.3.3 IONOSPHERE ERRORS

The free electrons in the ionosphere cause that navigation signals do not travel at the vacuum speed of light as they transit this region. The signal modulation (the code and data stream) is delayed in proportion to the number of free electrons encountered and is also proportional to the inverse of the carrier frequency squared ($1/f^2$), while the carrier phase is advanced by the same amount. Carrier-smoothed receivers should take this into account in the design of their filters. There are different models how to correct the pseudoranges for the ionospheric delay [58]:

- The simplest technique is to use the internal diurnal model of these errors (parameters can be updated via navigation message) – it provides about 2-5 m of accuracy for users in temperate zones of the world (i.e. where ionosphere is stable).
- The second technique (for dual-frequency receivers) is to measure signal at both L1 and L2 frequencies and use an algebraic solution directly - accuracy of this modelling is about 1-2 m.
- The third technique is just simply to rely on a real time update (i.e. WADGPS - Wide Area Differential GPS Systems) - accuracy of this modelling is also about 1-2 m.

10.3.4 TROPOSPHERE ERRORS

The main effects of the troposphere on GPS signals produced are attenuation, signal delay, and scintillation.

The troposphere is the lowest part of the atmosphere with a variable depth of 9 km at the poles to 16 km at the equator. It consists of dry gases (mainly N_2 and O_2) and water vapour, both with different pressure profiles.

The tropospheric delay is a function of the tropospheric refractive index that is dependent on several factors such as temperature, pressure and humidity – this causes variations in the speed of light of electromagnetic waves. The value of the refractive index near to the Earth's surface is slightly more than 1 thus the speed of the signal in the troposphere is slower than in vacuum. The refractive index does not depend on the frequency of the signal, the troposphere is non-dispersive at frequencies to 15 GHz and therefore the code and carrier have the same delay.

The majority of the signal delay (90 %) is the dry part of the troposphere that can be, fortunately, easily modelled. On the other hand, the wet part of the troposphere is difficult to predict. The delay effects on the GPS signals in range vary from 2 - 25 m (more in [58]).

Random amplitude and phase scintillations are caused by irregularities in the refractive index and depend on elevation angle and weather conditions. Tropospheric scintillations are relatively small except at low elevation angles.

With the use of tropospheric models (i.e. the Saastamoinen model or the Hopfield model), the total zenith delay error can be 5-10 cm [2].

10.3.5 MULTIPATH ERRORS

Multipath is the error caused by reflected signals arriving at the receiver via multiple paths and distorting not only the PRN code and navigation data, but also the real correlation peak. Under the worst case conditions, multipath can cause the receiver tracking loops to lose lock.

The multipath effect can be reduced by different techniques, discussed in more detail in chapter 3.

Typical multipath error can vary from 1 – 5 m in highly reflective environment. The corresponding errors in the carrier phase measurement are typically on the order of centimetres [2].

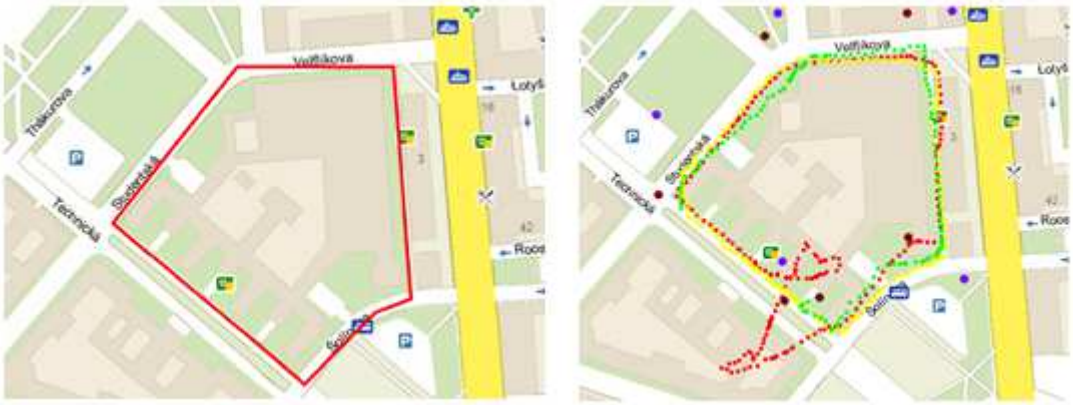

Figure 10. 1Illustration of errors in GNSS positioning in urban canyon

10.3.6 RECEIVER ERRORS

Most modern commercial receivers use five or six tracking channels on a single chip and reconstructed carrier to aid the code tracking loops. Inter-channel bias is minimized with digital sampling. This ensures a precision of better than 0.3 m [58].

11 3D ENVIRONMENT MODEL

3D reconstruction and texturing of buildings has become increasingly important for a number of applications and has been an active research topic in recent years. There is a variety of approaches with different resolutions, levels of accuracy, methods, completion times, stages and costs (e.g. laser scanners, photogrammetric approach). For more, see e.g. [59], [60].

Moreover, as 3D building models are becoming more geometrically accurate, they can truly be regarded as a new data source to improve the positioning accuracy in urban canyons. Research done in this dissertation focuses on these models to evaluate GNSS positioning performance with 3D ray tracing techniques. This can be achieved using satellite visibility and geometry predictions for any given location compared with measured satellite visibility to determine the user's current position.

This chapter deals with obtaining 3D geometry data from a real environment, extracting them into 3D modelling software, determining current satellites visibility above the user's receiver, and transforming their coordinates into the same units.

11.1 3D DATA VISUALIZATION

The most known 3D Geospatial Browser is Google Earth. Digital model or 3D representation of a terrain's surface is available in a Digital Elevation Model (DEM – a type of raster Geographic Information System GIS layer) format, albeit not that accurate for many areas [61].

Buildings visualized in Google Earth are usually created through 3D modelling software and imported as KML (Keyhole Markup Language) or KMZ (Keyhole Markup Language Zipped – a compressed version of a KML) file formats.

The representation of buildings in Google Earth is obtainable in a Boundary Representation Model (BREP). These models can also have textures associated with them. KML supports representation of objects by using the BREP method. The language is based on the XML standard and uses a tag-based structure with nested elements and attributes. In KML, building geometries are represented by polygons.

There are two distinct methods to represent the building geometries [61]. The first method defines a base polygon that corresponds to the floor plan of the building and extends it to the height of the building. The other method uses multiple polygons which allow more detailed geometrical representation of the building elements.

Other well-known 3D Geospatial Browsers are e.g. Microsoft Virtual Earth or NASA World Wind.

11.2 3D DATA EXTRACTION

There is no direct way to export the geometry with textures and coordinates mapped automatically. For my purpose, I used 3D Ripper DX to capture, import, and export given urban environment from Google Earth into Autodesk 3ds Max.

Capturing Google Earth Geometry

Steps to follow

Download and run Google Earth [S1, go to Tools > Options and set the Graphics Mode to DirectX, as illustrated in Figure 11. 1. Leave all other settings at default. Apply changes and close it.

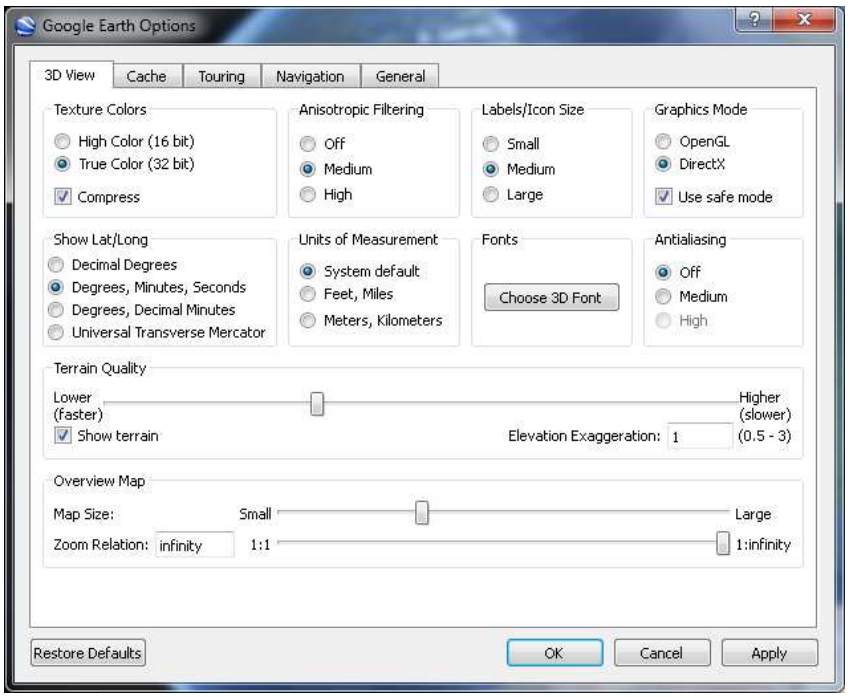

Figure 11. 1 Google Earth options set up

Download and run 3D Ripper DX [S2], tick checkbox and copy and paste Autodesk 3D Max 2011 path manually. Select googleearth.exe path ''*C:\Program Files (x86)\Google\Google Earth\client*", define Capture key and press the Launch button, as illustrated in Figure 11. 2.

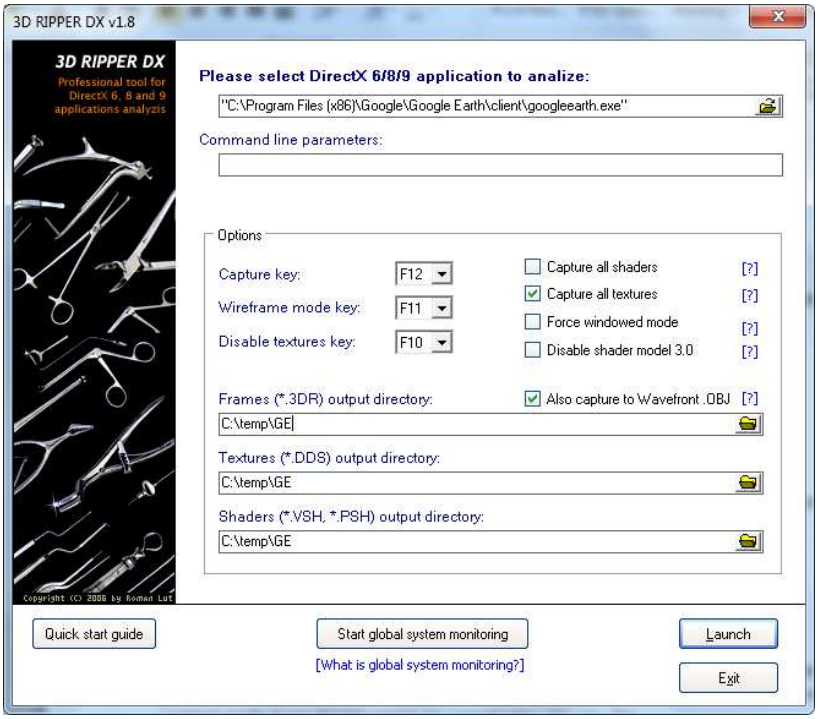

Figure 11. 2 3D Ripper DX options set up

In Google Earth, there is a *Ready to capture* yellow label displayed in the left corner. Go to the point of destination (i.e. Studentská street, Prague, Figure 11. 3 and Figure 11. 4). Click on North button on compass and press the Capture key. Exported data are stored in output directory defined in 3D Ripper DX Options.

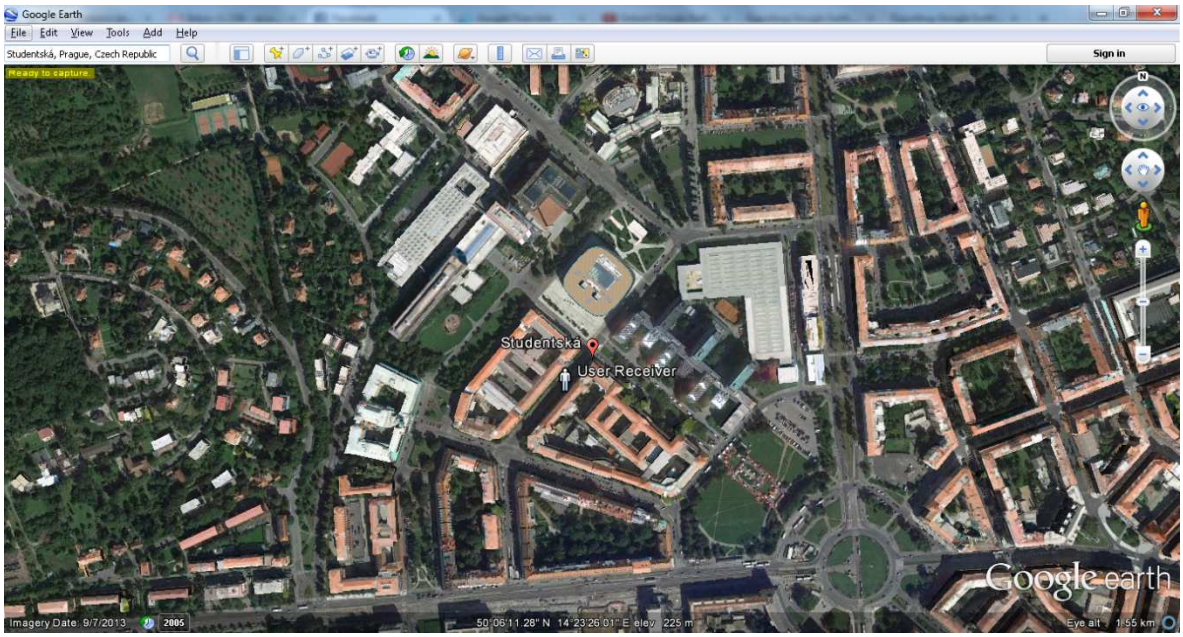

Figure 11. 3 Google Earth, Studentská street, Prague

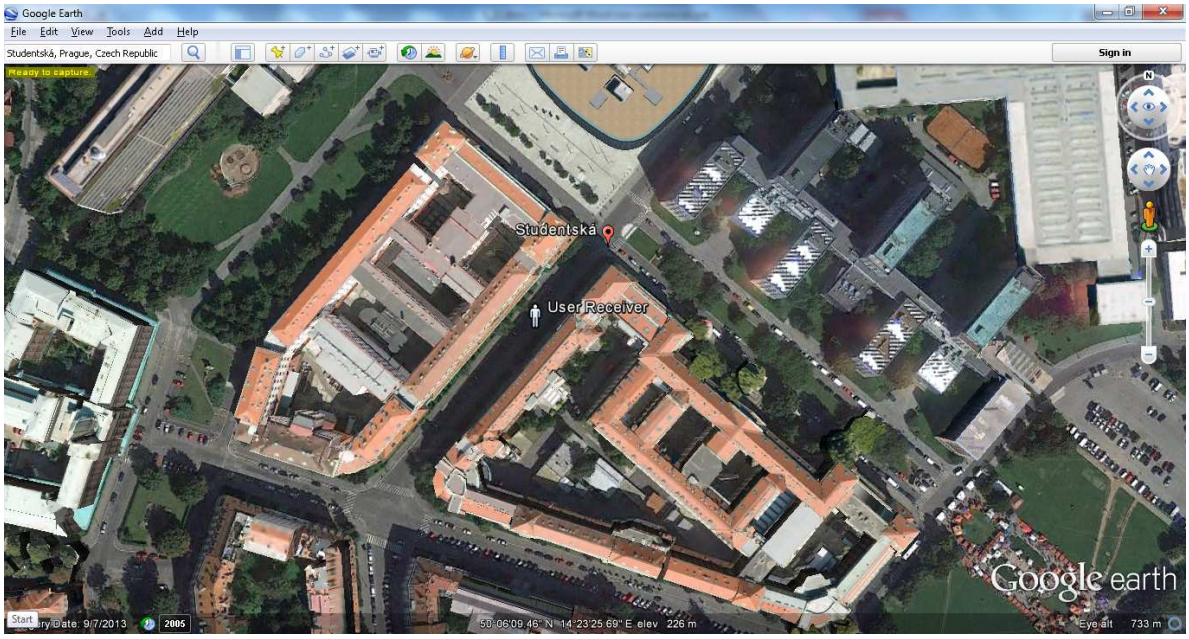

Figure 11. 4 Google Earth, Studentská street, Prague

Importing / exporting data from Autodesk 3ds Max 2011

Steps to follow

Download and run Autodesk 3ds Max 2011 [S3]. Import captured data in 3.dr file and change settings to:

- FOV: horizontal (for width) to 60 (defined for Google Earth)
- Monitor aspect ratio (for Google Earth): 1.58 (image size1025:646)

Group all data and scale it.

Export data into .obj file - the building layout is considered to be made up of triangles put together, as shown in Figure 11. 5.

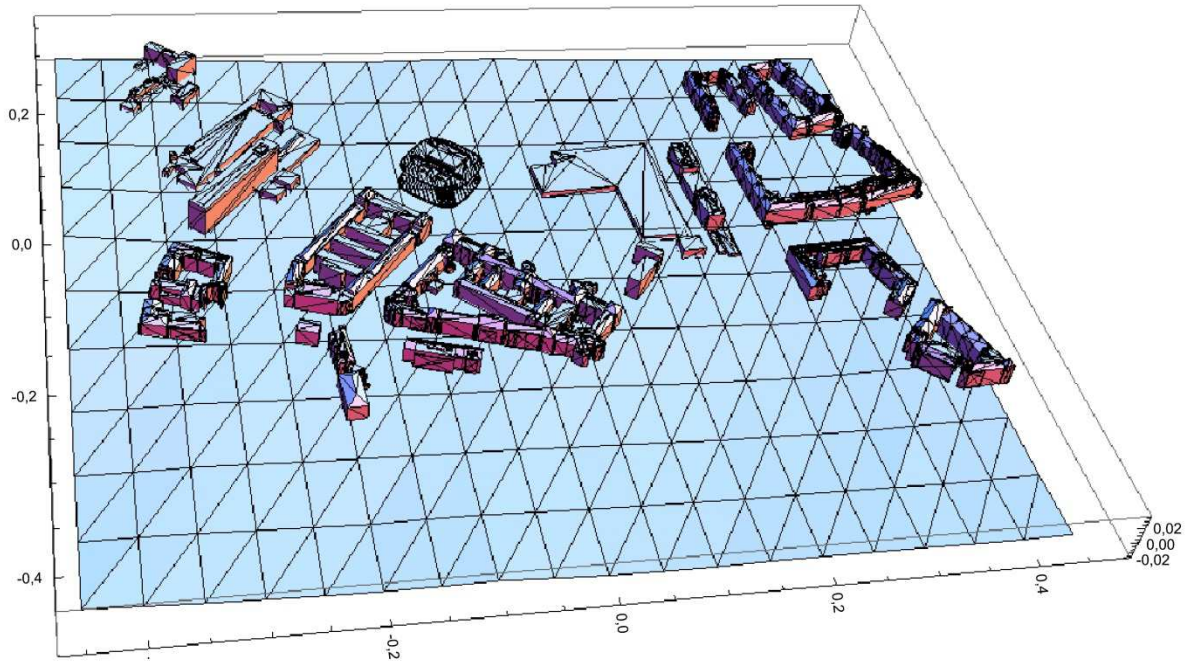

Figure 11. 5 Representation of building geometry of Studenstá street, Prague in .obj file

11.3 SATELLITE COORDINATES EXTRACTION

The information about which satellite is visible for a certain receiver in a 3D city model at a certain time is found in GNSS almanac data[3], e.g. an example in Table 11. 1 below [62]. Satellite coordinates are computed in Earth-centred, Earth-fixed (ECEF) WGS-84 coordinates.

11.4 SATELLITE COORDINATES TRANSFORMATION

The position of the receiver is reported in mapping coordinates ($Xm,\ Ym,\ Zm$ – the same coordinate system when extracting building geometry from Google Earth). The satellite position coordinates are in different units.

The transfer matrix between these two coordinate systems is as follows:

$$M_{ECEF\_MC} = \begin{bmatrix} -\sin\beta & \cos\beta & 0 \\ -\cos(\beta) * \sin(\alpha) & -\sin(\beta) * \sin(\alpha) & \cos(\alpha) \\ \cos(\alpha) * \cos(\beta) & \cos(\alpha) * \sin(\beta) & \sin(\alpha) \end{bmatrix}, \qquad (11.\ 1)$$

where α and β respectively represent latitude (N) and longitude (E) coordinates converted to radians.

[3] The Extended Standard Product 3 Orbit Format (SP3-c): http://igscb.jpl.nasa.gov/igscb/data/format/sp3c.txt.

SV Id	x-axis (km)	y-axis (km)	z-axis (km)	clock (μs)	x-sdev (mm)	y-sdev (mm)	z-sdev (mm)	c-sdev (psec)
PG01	18727.3526	13392.45369	-13438.5366	-9.926704	8	7	8	265
PG02	4999.30643	-15107.8031	21571.08488	543.173994	10	7	8	215
PG03	13310.9034	21493.73447	8071.977401	162.30281	10	8	2	276
PG04	8836.98396	16153.068	-19545.3491	-5.962715	10	10	8	208
PG05	-811.110948	-24454.4119	10057.39697	-289.89872	10	6	6	204
PG06	19568.8046	-7683.8845	16213.01606	57.816215	12	10	7	267
PG07	25705.8677	7169.831219	2021.352151	433.450583	7	10	9	198
PG08	-3852.30712	14043.27973	22413.62401	17.221874	12	9	10	218
PG09	17663.0275	906.782514	19810.08501	-61.910058	8	10	5	233
PG10	12375.9121	-10434.5418	20609.58649	-159.73861	7	8	8	224
PG11	13060.5004	13755.87857	-19164.182	-552.35433	8	10	6	184
PG12	-10652.7771	-23839.0867	5392.24104	263.072656	10	9	7	201
PG13	9629.16124	-21040.3559	-13300.5917	-80.820987	11	10	8	202
PG14	-21144.3156	14469.93556	-6480.63526	94.798279	11	10	8	196
PG15	-4821.53123	-17201.2607	-19641.4633	-227.61479	13	11	3	207
PG16	-462.831726	24235.40046	10349.1393	-163.13874	11	6	11	187
PG17	20983.6307	-13441.7467	-8574.69122	-151.232	10	10	8	225
PG18	-17196.8887	-5008.9432	-19229.9273	373.851948	10	7	8	165
PG19	-1712.2582	19040.11596	-18412.9574	-497.48712	11	9	10	177
PG20	17900.9581	8642.979347	17506.72733	281.060387	10	9	6	212
PG21	-26425.9391	-3227.90678	-2196.02216	-407.95858	10	10	11	188
PG22	-13278.9832	9478.526994	-20722.8724	309.712364	7	9	9	207
PG23	10972.3514	11001.53879	21659.49734	-83.233803	9	11	7	188
PG24	-16094.4187	-14254.0457	-15709.272	-42.14888	9	11	6	212
PG25	-16066.944	-14091.0338	15791.80009	1.808246	9	11	9	192
PG27	-10305.0379	22313.6914	-9964.69215	45.858861	11	9	11	191
PG28	13909.0568	-3457.74168	-21739.726	413.986324	9	13	8	199
PG29	-15537.6843	-4645.44613	21056.3882	587.280916	6	9	8	199
PG30	25069.9783	526.512314	-8827.5337	-86.338459	12	11	8	256
PG31	-17703.7819	8506.585502	18181.61394	325.028779	14	10	11	206
PG32	3885.10572	26324.95509	-3634.39025	-242.50836	9	9	9	219

Table 11. 1 Example 1 – position and lock record – 21.1.2015 12:15:00

12 MULTIPATH DETECTION MODEL FOR DYNAMIC PROPAGATION ENVIRONMENTS

In the following, the proposed multipath detection model for dynamic propagation environments is presented.

Generally, direct (i.e. line-of-sight, LOS) signal is normally the most wanted signal. Nevertheless signals can also arrive at a receiver via a number of different paths that may occur between a satellite and a receiver. These paths are results of reflections and diffractions from buildings, water, ground etc.

To investigate whether GNSS signals have arrived at a receiver directly or through reflections, the ray-tracing algorithm is introduced based on information obtained from 3D buildings model, assumed position of the receiver, and known position of GNSS satellites extracted from the navigation message.

In section 12.1, calculation of the direct path between the satellite and the receiver is described. In section 12.2 and section 12.3, single reflection and multiple reflections of a GNSS signal are calculated, and the coordinates of reflection points are determined. Thus, in section 12.4 the reflection length (or the signal path delay) is computed.

All MATLAB code ([S4], [S5]) can be found on the supplemented CD attached to the inside back cover.

12.1 CALCULATION OF DIRECT PATH

Consider a ray $\overrightarrow{\mathbf{SP}}$ from S (satellite) to P (receiver), and a triangle with vertices A, B, C (obtained from the 3D map), as illustrated in Figure 12. 1.

12.1.1 LINEARLY INDEPENDENT VECTORS

To avoid all points *(S, P, A, B, C)* being on the same line, the algorithm provides an estimate of the number of linearly independent vectors $\overrightarrow{\mathbf{AB}}$, $\overrightarrow{\mathbf{BC}}$ and $\overrightarrow{\mathbf{SP}}$. They are linearly independent if none of them can be expressed as a linear combination of the others, otherwise they are dependent and the algorithm does not consider them in further calculations.

Let $A = \{\overrightarrow{\mathbf{AB}}, \overrightarrow{\mathbf{BC}}, \overrightarrow{\mathbf{SP}}\}$ be a collection of vectors from R^3. Then the vectors are said to be linearly independent if [63]:

$$rank\ (A) = 3. \tag{12. 1}$$

(MATLAB function called *obstruction_in_view.m*).

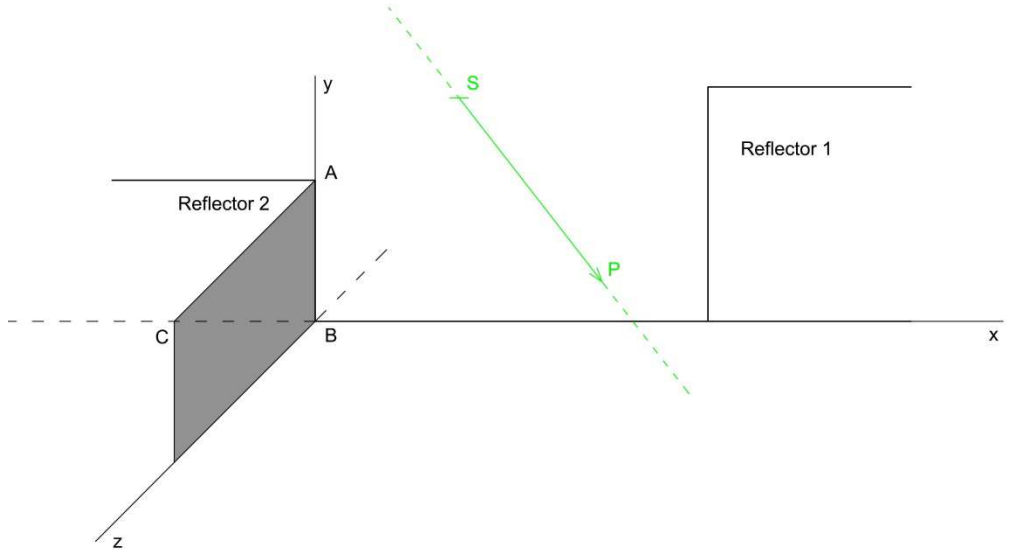

Figure 12. 1 Illustration of GNSS signal – direct path

12.1.2 LINE-OF-SIGHT BETWEEN TWO POINTS

To get the intersection of the vector $\overrightarrow{\mathbf{SP}}$ with the $\triangle \mathrm{ABC}$, we first determine the intersection of the vector $\overrightarrow{\mathbf{SP}}$ and the plane ρ ($\triangle \mathrm{ABC} \in \rho$), more in section 12.1.3. If it does not intersect, then it also does not intersect the $\triangle \mathrm{ABC}$ and the time and distance from the satellite to the receiver are calculated from pseudoranges, as in the equation (9. 3).

However, if they do intersect in the point *R* (reflection), we need to determine if this point is inside the $\triangle \mathrm{ABC}$, more in section 12.2.

A limitation is done to exclude the intersection point *R* as a part of the ray $\overrightarrow{\mathbf{SP}}$ ($\mathrm{R} \notin \overrightarrow{\mathbf{SP}}$).

(MATLAB function called *line_of_sight.m*).

(MATLAB function called *pseudoranges_computation.m*).

(MATLAB function called *distance.m*).

12.1.3 INTERSECTION OF A RAY WITH A PLANE

A plane is defined by three non-collinear points (three points not on a line) $A,\ B,\ C \in \mathrm{R}^3$. These three points define two distinct vectors $\overrightarrow{\mathbf{AB}}$ and $\overrightarrow{\mathbf{AC}}$. The $\triangle \mathrm{ABC}$ lies in the plane ρ through A with normal vector $\vec{\mathbf{w}}$ [50]:

$$\vec{\mathbf{w}} = \overrightarrow{\mathbf{AB}} \times \overrightarrow{\mathbf{AC}}. \qquad (12.\ 2)$$

Then the parametric plane equation through a point is:

$$\mathbf{R} = \mathbf{A} + (\mathbf{B} - \mathbf{A}) \cdot s + (\mathbf{C} - \mathbf{A}) \cdot u, \tag{12. 3}$$

where $s, u \in \mathrm{R}$.

The parametric equation of a ray that passes through a point is:

$$\mathbf{R} = \mathbf{P} + (\mathbf{P} - \mathbf{S}) \cdot t, \tag{12. 4}$$

where $t \in \mathrm{R}$.

By inserting equation (12. 3) to equation (12. 4), we get the solution to t, s, u:

$$\mathbf{M}_{\mathbf{t,s,u}} = \left[\begin{array}{ccc|c} S_x - P_x & B_x - A_x & C_x - A_x & P_x - A_x \\ S_y - P_y & B_y - A_y & C_y - A_y & P_y - A_y \\ S_z - P_z & B_z - A_z & C_z - A_z & P_z - A_z \end{array}\right]. \tag{12. 5}$$

By substituting the solution of equation (12. 5) into equation (12. 3) or equation (12. 4), we get the parametric coordinates of the intersection point R in the plane.

(MATLAB function called *obstruction_in_view.m*).

12.2 CALCULATION OF SINGLE REFLECTION

Further, different models of reflection are considered. First, a single reflection model is described, as illustrated in Figure 12. 2.

12.2.1 INTERSECTION OF A POINT AND A PLANE

The basic criteria to determine whether a point R_1 lies inside a triangle defined with vertices A, B, C or not is as [50], [62]:

$$\alpha_1 + \alpha_2 + \alpha_3 = 1, \tag{12. 6}$$

$$\alpha_1, \alpha_2, \alpha_3 \geq 0, \tag{12. 7}$$

$$\alpha_1 \mathbf{A} + \alpha_2 \mathbf{B} + \alpha_3 \mathbf{C} = \mathbf{R_1}, \tag{12. 8}$$

where $R_1, A, B, C \in \mathrm{R}^3$; $\alpha_1, \alpha_2, \alpha_3 \in \mathrm{R}$. In other words, the point R_1 has to be a convex combination of the $\triangle \mathrm{ABC}$.

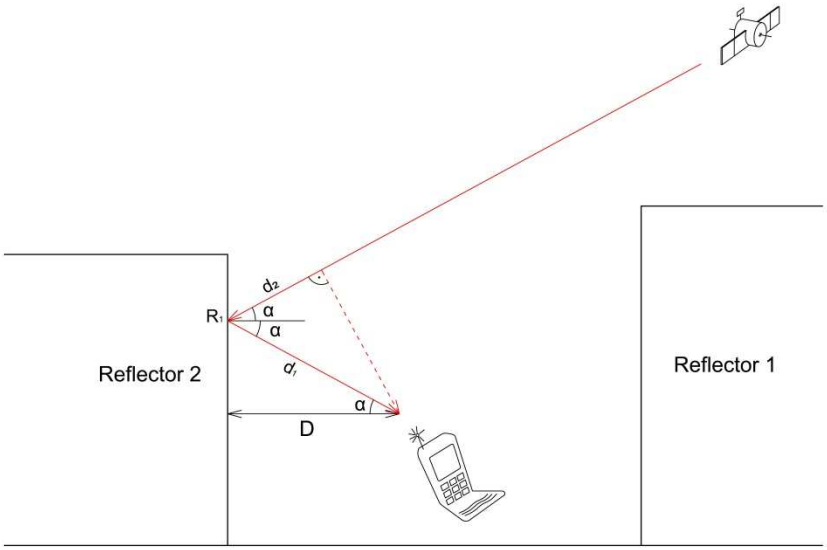

Figure 12. 2 Illustration of single reflection on a planar reflector

Given the point R_1 and the $\triangle$ABC, we find the solution to $\alpha_1, \alpha_2, \alpha_3$:

$$\mathbf{M}_{\alpha_1,\alpha_2,\alpha_3} = \left[\begin{array}{cccc} 1 & 1 & 1 & 1 \\ A_x & B_x & C_x & R_{1x} \\ A_y & B_y & C_y & R_{1y} \\ A_z & B_z & C_z & R_{1z} \end{array}\right]. \quad (12.\ 9)$$

To determine whether the intersection point R_1 does or does not lie inside the $\triangle$ABC, the algorithm verifies the conditions described in equation (12. 6), equation (12. 7) and gives the solution.

(MATLAB function called *intersection_of_point_and_plane.m*).

12.2.2 SINGLE REFLECTION PATH - ONE POINT OF REFLECTION

The equation for the plane ABC going through the point A is as [64]:

$$w_x A_x + w_y A_y + w_z A_z + d = 0\ , \quad (12.\ 10)$$

where $\vec{\mathbf{w}}$ is the normal vector for the plane ABC defined in equation (12. 2).

It is assumed that the reflected point R_1 is part of lines $|\mathrm{SR_1}|$ (defines the distance from the satellite S to the reflected point R_1), $|\mathrm{R_1P}|$ (defines the distance from the reflected point R_1 to the known position of the receiver), and the plane ABC. Its coefficients are described by the normal vector $\vec{\mathbf{w}}$.

Therefore, any reflected point R_1 on the plane ABC satisfies the normal implicit equation:

$$\vec{\mathbf{w}} \cdot (\mathbf{R_1} - \mathbf{A}) = 0\,, \tag{12. 11}$$

and as in equation (12. 4), the reflection point R_1 can be expressed also by:

$$\mathbf{S} + \overrightarrow{\mathbf{n_1}}\,.\,t_1 = \mathbf{P} + \overrightarrow{\mathbf{n_2}}\,.\,t_2\,, \tag{12. 12}$$

where S defines the known satellite position, P represents the assumed position of the receiver, $t_1, t_2 \in \mathrm{R}$, $\overrightarrow{\boldsymbol{n_1}}$ is the directional vector of the line $|\mathrm{SR_1}|$, $\overrightarrow{\boldsymbol{n_2}}$ is the directional vector of the line $|\mathrm{R_1P}|$.

The relation between these two directional vectors is given by:

$$\overrightarrow{\mathbf{n_2}} = \overrightarrow{\mathbf{n_1}} \times \mathbf{M_{REF}}\,, \tag{12.13}$$

where $\mathbf{M_{REF}}$ is the matrix describing reflection:

$$\mathbf{M_{REF}} = -inv\begin{bmatrix} \mathbf{w} \\ \mathbf{A}-\mathbf{B} \\ \mathbf{A}-\mathbf{C} \end{bmatrix} * \begin{bmatrix} -1 & 0 & 0 \\ 0 & 1 & 0 \\ 0 & 0 & 1 \end{bmatrix} * \begin{bmatrix} \mathbf{w} \\ \mathbf{A}-\mathbf{B} \\ \mathbf{A}-\mathbf{C} \end{bmatrix}, \tag{12.14}$$

Now we know whether there is a path with a single reflection between the satellite and the receiver. If so, the algorithm gives coordinates (X, Y, Z) of the reflected point $R_1 \in \mathrm{R}^3$ as a result.

(MATLAB function called *one_point_of_reflection.m*).

(MATLAB function called *single_reflection_path.m*).

12.3 CALCULATION OF MULTIPLE REFLECTIONS

GNSS availability in urban environment is seriously degraded by buildings blocking direct signals from more than one side, as illustrated in Figure 12. 3.

12.3.1 TWO REFLECTIONS PATH – TWO POINTS OF REFLECTION

Now when we know the reflection matrix, we can simply calculate if a GNSS signal arrived at the receiver via more than one reflection. The principle is similar: for the second reflection, the plane $A_2B_2C_2$, with normal vector $\overrightarrow{\mathbf{w_2}}$ is defined.

The equation for the plane $A_2B_2C_2$ going through the point A_2 is as [64]:

$$w_{2x}A_{2x} + w_{2y}A_{2y} + w_{2z}A_{2z} + d_2 = 0. \tag{12. 15}$$

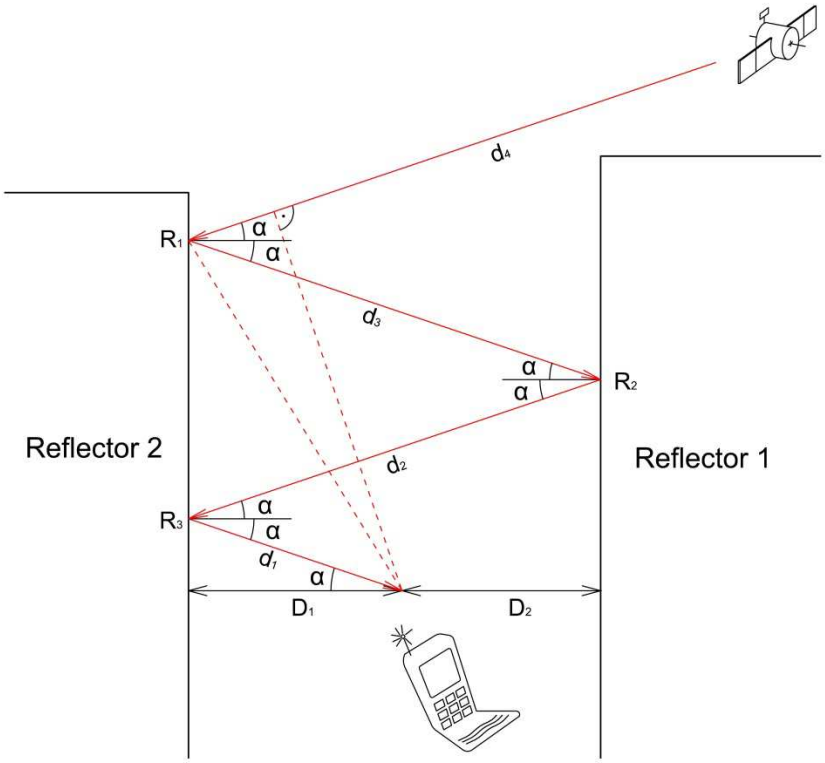

Figure 12. 3 Illustration of multiple reflections in planar reflectors

Similar to the equation (12. 4), the second reflection point R_2 can be expressed by:

$$\mathbf{R_1} + \overrightarrow{\mathbf{n_2}} \cdot t_2 = \mathbf{P} + \overrightarrow{\mathbf{n_3}} \cdot t_3 \,, \tag{12.16}$$

where $t_2, t_3 \in \mathrm{R}$, $\overrightarrow{\mathbf{n_2}}$ is the directional vector of the line $|\mathrm{RR_2}|$, $\overrightarrow{\mathbf{n_3}}$ is the directional vector of the line $|\mathrm{R_2P}|$.

The relation between the directional vectors $\overrightarrow{\mathbf{n_3}}$ and $\overrightarrow{\mathbf{n_1}}$ is given by:

$$\overrightarrow{\mathbf{n_3}} = \overrightarrow{\mathbf{n_1}} \times \mathbf{M_{2\_REF}} \,, \tag{12.17}$$

where $\mathbf{M_{REF}}$ is the matrix describing the first reflection, $\mathbf{M_{2\_REF}}$ is the matrix describing the second reflection:

$$\mathbf{M}_{2\_\mathbf{REF}} = \mathbf{M}_{\mathbf{REF}} * \left[-inv \begin{bmatrix} \mathbf{w}_2 \\ \mathbf{A}_2 - \mathbf{B}_2 \\ \mathbf{A}_2 - \mathbf{C}_2 \end{bmatrix} * \begin{bmatrix} -1 & 0 & 0 \\ 0 & 1 & 0 \\ 0 & 0 & 1 \end{bmatrix} * \begin{bmatrix} \mathbf{w}_2 \\ \mathbf{A}_2 - \mathbf{B}_2 \\ \mathbf{A}_2 - \mathbf{C}_2 \end{bmatrix} \right], \tag{12.18}$$

(MATLAB function called *two_points_of_reflection.m*).

(MATLAB function called *two_reflections_path.m*).

For more reflections, the principle is the same. Generally, every side of a building is

defined by a plane with a normal vector. This normal vector describes every point on a plane, therefore also the reflected point. Relations between directional vectors of all lines and planes are described by matrixes.
(MATLAB function called *three_points_of_reflection.m*).
(MATLAB function called *four_points_of_reflection.m*).
(MATLAB function called *five_points_of_reflection.m*).

12.4 CALCULATION OF THE REFLECTION LENGTH

12.4.1 CALCULATION OF SINGLE REFLECTION LENGTH

Given by known coordinates of S, R_1, and P (as in Figure 12. 2), the reflection length for a single reflection can be simply calculated as:

$$D = d_1 + d_2 \,, \tag{12. 19}$$

where d_1 is $|\mathrm{PR}_1|$, and d_2 is $|\mathrm{SR}_1|$ in meters.

As in the equation (9. 3), the distances d_1 and d_2 are calculated as:

$$d_1 = \sqrt{(R_{1x} - P_x)^2 + \left(R_{1y} - P_y\right)^2 + (R_{1z} - P_z)^2} \,, \tag{12. 20}$$

$$d_2 = \sqrt{(R_{1x} - S_x)^2 + \left(R_{1y} - S_y\right)^2 + (R_{1z} - S_z)^2}. \tag{12. 21}$$

From the knowledge that GNSS signals travel at the speed of light and the known distance to the receiver, we can simply calculate the time the signal took to reach the receiver.

The benefit of a single reflection is that after reflection, the circular polarization of a GNSS signal is changed to left-handed (LHCP). An RHCP antenna can supress the LHCP reflection quite effectively so the multipath reflection error is minimised. Naturally, a second reflection will cause the RHCP polarization again [65], [66], [67].

(MATLAB function called *distance_with_one_point_of_reflection.m*).
(MATLAB function called *distance.m*).

12.4.2 CALCULATION OF MULTIPLE REFLECTIONS LENGTH

The distance for multiple reflections, i.e. three points of reflection (as in Figure 12. 3), can be simply calculated as:

$$D = d_1 + d_2 + d_3 + d_4 \,, \tag{12. 22}$$

where d_1 is $|PR_3|$, d_2 is $|R_2R_3|$, d_3 is $|R_1R_2|$, d_4 is $|SR_1|$ in meters. S, R_1, R_2, R_3 and $P \in R^3$ and their coordinates are known.

As in equation (9. 3), the distances d_1, d_2, d_3 and d_4 are calculated as:

$$d_1 = \sqrt{(R_{3x} - P_x)^2 + \left(R_{3y} - P_y\right)^2 + (R_{3z} - P_z)^2}\,, \tag{12. 23}$$

$$d_2 = \sqrt{(R_{3x} - R_{2x})^2 + \left(R_{3y} - R_{2y}\right)^2 + (R_{3z} - R_{2z})^2}\,, \tag{12. 24}$$

$$d_3 = \sqrt{(R_{2x} - R_{1x})^2 + \left(R_{2y} - R_{1y}\right)^2 + (R_{2z} - R_{1z})^2}\,, \tag{12. 25}$$

$$d_4 = \sqrt{(R_{1x} - S_x)^2 + \left(R_{1y} - S_y\right)^2 + (R_{1z} - S_z)^2}. \tag{12. 26}$$

From the knowledge that GNSS signals travel at the speed of light and the known distance to the receiver, we can calculate the time the signal took to reach the receiver.

(MATLAB function called *distance_with_two_points_of_reflection.m*).
(MATLAB function called *distance.m*), etc.

13 DETECTION OF A USER'S POSITION

It is evident that if it is possible to calculate the total propagation path length of the GNSS signals – using intelligent maps and other data – then it is also possible to perform the order of operations in reverse and thus to determine the actual, unknown position of the user.

The principle is described as a sequence of following steps:

- determining the number of satellites visible using a combination of intelligent maps and known position of the subject;
- performing calculations to determine the position (the position in a presumed region) if the number of satellites that are in direct line-of-sight is greater than or equal to three;
- based on combination of intelligent maps data (including terrain and buildings height) and measured GNSS data (with known positions of satellites obtained from navigation message) – the final position of the receiver is found;

Typical application of a new method of determining the position is as follows:

The user is equipped with a GNSS receiver able to plan and define the route where he moves along. In a simple environment the position of the user is displayed on the map inside the planned rout. In a complex environment this may not be obvious thanks to the influence of reflections of GNSS signals. In the case the position of the user (measured data from the GNSS receiver) is displayed outside the planned route, it is necessary to define his true position. This means to find such a point in the specified interval (defined by his last known position and the place he is able to reach) using the multipath propagation model which gives the same position as the measured data from the GNSS receiver. If this succeeds, the position obtained from the model is identical to the actual user's position. For speeding up calculations, the interval halving method can be used, repeating iterations in so many steps until an agreement between measured and calculated parameters is reached.

Detailed description of individual steps can be found in chapter 2 and chapter 15.

14 FUNCTION CALL GRAPH

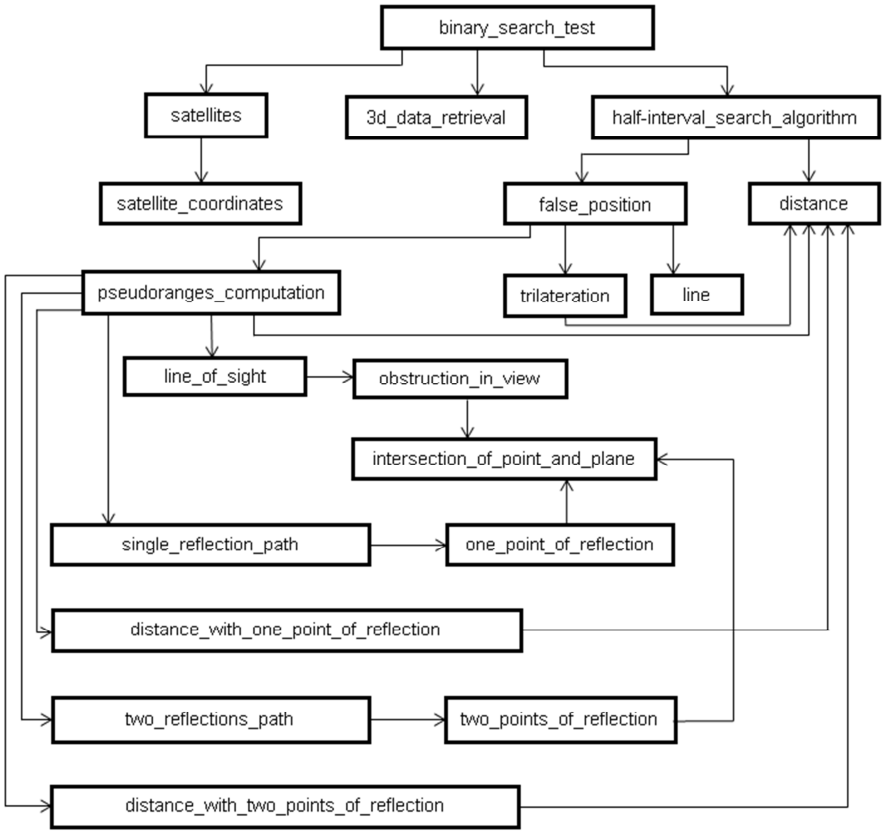

Figure 14. 1 Call graph

binary_search_test

The output of the whole program is the new expected position of the user in the selected area. The calculation is based on the following: digital 3D maps information, known positions of GNSS satellites, and an assumed position of a receiver. Individual functions are described below in the same order as shown in the call graph above. All MATLAB code can be found on the supplemented CD attached to the inside back cover.

(MATLAB script called *binary_search_test.m*).

3d_data_retrieval

At first the program reads .cvs geometry data in the form of ABC triangles and their coordinates represented in the mapping coordinate system in meters. Data can be limited if necessary.

(MATLAB script called *3d_data_retrieval.m*).

satellites

Then the program retrieves data from the navigation message, for our purposes the satellite coordinates which are first transferred into the mapping coordinate system via transfer matrix described in equation 10. 1. Data are represented in meters; for faster evaluation, the selection can be limited only to the satellites which find themselves above the horizon.

(MATLAB script called *satellites.m*).

satellite_coordinates

The transfer matrix between these two coordinate systems is described in this function.

(MATLAB function called *satellite_coordinates.m*).

half-interval search algorithm

The output of this function is the final position of the user. The function is called from the *binary_search_test*.*m*.

(MATLAB function called *half-interval_search_algorithm.m*).

false_position

This function identifies the false position of the user. For this position the current GNSS signal propagation is determined.

(MATLAB function called *false_position.m*).

distance

This function calculates the distance between two points on the three dimensions of the *xyz*-plane, as described in equation (9. 3).

(MATLAB function called *distance.m*).

pseudoranges_computation

This function evaluates the ray-tracing model for a simulation of GNSS signals reception in urban canyons as described in chapter 12. The result is the information on which signals from which satellites were received directly and which signals were received via reflections. It also calculates the time needed for transmission for each signal.

The following data is used as an input: known positions of GNSS satellites, assumed position of a receiver, 3D maps information, and satellites IDs.

(MATLAB function called *pseudoranges_computation.m*).

trilateration

This function is called from *false_position.m*. It is used to determine the receiver position on the Earth's surface by timing signals from satellites.

(MATLAB function called *trilateration.m*).

line

This function defines a line between two points. It is not used for any calculations, only for the purpose of illustration.

(MATLAB function called *line.m*).

line_of_sight

This function determines whether there is a line of sight between two points or an obstacle in between the two points.

(MATLAB function called *line_of_sight.m).*

single_reflection_path

This function determines whether there is a path with single reflection between two points.

(MATLAB function called *single_reflection_path.m*).

distance_with_one_point_of_reflection

If there is a single reflection between the two points, the function calculates the final distance between them.

(MATLAB function called *distance_with_one_point_of_reflection.m*).

two_reflections_path

This function determines whether the satellite signal arrived at the receiver via two reflections.

(MATLAB function called *two_reflections_path.m*).

distance_with_two_points_of_reflection

If there are two reflections on the path from the satellite to the receiver, the function calculates the final distance between them.

(MATLAB function called *distance_with_two_points_of_reflection.m*).

obstruction_in_view

The output of this function is the information whether a ray defined with points *S* (satellite), *P* (receiver), and a triangle ABC defined with vertices A, B, C are linearly independent. In other words, it prevents all points (*S, P, A, B, C*) from lying on the same line.

(MATLAB function called *obstruction_in_view.m*).

intersection_of_point_and_plane

This function determines whether a point is a part of a given triangle ABC.

(MATLAB function called *intersection_of_point_and_plane.m*).

one_point_of_reflection

This function determines the single reflection point and its coordinates.

(MATLAB function called *one_point_of_reflection.m*).

two_points_of_reflection

This function determines two points of reflection and their coordinates.

(MATLAB function called *two_points_of_reflection.m*).

Implementation – one_point_of_reflection

```
function [out,X1] =one_point_of_reflection(A,B,C,X0,Xn)
u = (B-A)';
v = (C-A)';
w = linsolve([u;v;[1,pi,exp(1)]],[0;0;1]);
d=-w'*A;
eq0x = strcat(['x0x = ', num2str(X0(1))]);
eq0y = strcat(['x0y = ', num2str(X0(2))]);
eq0z = strcat(['x0z = ', num2str(X0(3))]);
eqnx = strcat(['xnx = ', num2str(Xn(1))]);
eqny = strcat(['xny = ', num2str(Xn(2))]);
eqnz = strcat(['xnz = ', num2str(Xn(3))]);
eq1 = strcat([num2str(w(1)),'*x1x','+',num2str(w(2)),'*x1y','+',num2str(w(3)),'*x1z = ', num2str(-d)]);
eq2 = 'x0x + n1 = x1x';
eq3 = 'x0y + n2 = x1y';
eq4 = 'x0z + n3 = x1z';
baze = [w,u',v']';
M = -inv(baze)*[-1, 0, 0;0,1,0;0,0,1]*baze;
eqM11 = strcat('M11=',num2str(M(1,1)));
eqM12 = strcat('M12=',num2str(M(1,2)));
eqM13 = strcat('M13=',num2str(M(1,3)));
eqM21 = strcat('M21=',num2str(M(2,1)));
eqM22 = strcat('M22=',num2str(M(2,2)));
eqM23 = strcat('M23=',num2str(M(2,3)));
eqM31 = strcat('M31=',num2str(M(3,1)));
eqM32 = strcat('M32=',num2str(M(3,2)));
eqM33 = strcat('M33=',num2str(M(3,3)));
eq5 = 'xnx + t2*(n1 * M11 + n2*M21 + n3*M31) = x1x';
eq6 = 'xny + t2*(n1 * M12 + n2*M22 + n3*M32) = x1y';
eq7 = 'xnz + t2*(n1 * M13 + n2*M23 + n3*M33) = x1z';
res =
solve(eq0x,eq0y,eq0z,eq1,eq2,eq3,eq4,eq5,eq6,eq7,eqM11,eqM12,eqM13,eqM21,eqM22,…
...eqM23,eqM31,eqM32,eqM33,eqnx,eqny,eqnz);
X1 = double([res.x1x,res.x1y,res.x1z])';
X1 = X1(:,1);
out = intersection_of_point_and_plane(X1,A,B,C);
end
```

Table 14. 1 One point of reflection implementation in Matlab

Implementation – two_points_of_reflection

```
function [out,X1,X2] = two_points_of_reflection(A,B,C,A2,B2,C2,X0,Xn)
u = (B-A)';
v = (C-A)';
w = linsolve([u;v;[1,pi,exp(1)]],[0;0;1]);
d=-w'*A;
u2 = (B2-A2)';
v2 = (C2-A2)';
w2 = linsolve([u2;v2;[1,pi,exp(1)]],[0;0;1]);
d2=-w2'*A2;
eq0x = strcat(['x0x = ', num2str(X0(1))]);
eq0y = strcat(['x0y = ', num2str(X0(2))]);
eq0z = strcat(['x0z = ', num2str(X0(3))]);
eqnx = strcat(['xnx = ', num2str(Xn(1))]);
eqny = strcat(['xny = ', num2str(Xn(2))]);
eqnz = strcat(['xnz = ', num2str(Xn(3))]);
eq1 = strcat([num2str(w(1)),'*x1x','+',num2str(w(2)),'*x1y','+',num2str(w(3)),'*x1z = ', num2str(-d)]);
eq1_2 = strcat([num2str(w2(1)),'*x2x','+',num2str(w2(2)),'*x2y','+',num2str(w2(3)),'*x2z = ', num2str(-
d2)]);
eq2 = 'x0x + n1 = x1x';
eq3 = 'x0y + n2 = x1y';
eq4 = 'x0z + n3 = x1z';
baze = [w,u',v']';
M = -inv(baze)*[-1, 0, 0;0,1,0;0,0,1]*baze;
baze2 = [w2,u2',v2']';
M2 = M*(-inv(baze2)*[-1, 0, 0;0,1,0;0,0,1]*baze2);
eqM11 = strcat('M11=',num2str(M(1,1)));
eqM12 = strcat('M12=',num2str(M(1,2)));
eqM13 = strcat('M13=',num2str(M(1,3)));
eqM21 = strcat('M21=',num2str(M(2,1)));
eqM22 = strcat('M22=',num2str(M(2,2)));
eqM23 = strcat('M23=',num2str(M(2,3)));
eqM31 = strcat('M31=',num2str(M(3,1)));
eqM32 = strcat('M32=',num2str(M(3,2)));
eqM33 = strcat('M33=',num2str(M(3,3)));
eqM11_2 = strcat('M11_2=',num2str(M2(1,1)));
eqM12_2 = strcat('M12_2=',num2str(M2(1,2)));
eqM13_2 = strcat('M13_2=',num2str(M2(1,3)));
eqM21_2 = strcat('M21_2=',num2str(M2(2,1)));
eqM22_2 = strcat('M22_2=',num2str(M2(2,2)));
eqM23_2 = strcat('M23_2=',num2str(M2(2,3)));
eqM31_2 = strcat('M31_2=',num2str(M2(3,1)));
eqM32_2 = strcat('M32_2=',num2str(M2(3,2)));
eqM33_2 = strcat('M33_2=',num2str(M2(3,3)));
eq5 = 'x2x + t2*(n1 * M11 + n2*M21 + n3*M31) = x1x';
```

```
eq6 = 'x2y + t2*(n1 * M12 + n2*M22 + n3*M32) = x1y';
eq7 = 'x2z + t2*(n1 * M13 + n2*M23 + n3*M33) = x1z';
eq5_2 = 'xnx + t3*(n1 * M11_2 + n2*M21_2 + n3*M31_2) = x2x';
eq6_2 = 'xny + t3*(n1 * M12_2 + n2*M22_2 + n3*M32_2) = x2y';
eq7_2 = 'xnz + t3*(n1 * M13_2 + n2*M23_2 + n3*M33_2) = x2z';
res = solve(eq0x,eq0y,eq0z,eq1,eq2,eq3,eq4,eq5,eq6,eq7,eqM11,eqM12,eqM13,eqM21,eqM22,…
...eqM23,eqM31,eqM32,eqM33,eqnx,eqny,eqnz,eq1_2,eq5_2,eq6_2,eq7_2,eqM11_2,eqM12_2,…
...eqM13_2,eqM21_2,eqM22_2,eqM23_2,eqM31_2,eqM32_2,eqM33_2);
X1 = double([res.x1x';res.x1y';res.x1z']);
X2 = double([res.x2x';res.x2y';res.x2z']);
for i=size(X1,2)
   out =intersection_of_point_and_plane(X1(:,i),A,B,C) & intersec-
tion_of_point_and_plane(X2(:,i),A2,B2,C2);
   if out
      break;
   end
end
```

Table 14. 2 Two points of reflection implementation in Matlab

15 RESULTS OF THE EXPERIMENTS

In this section, the method evaluation and results are presented. The ray-tracing algorithm is generally designed for different combinations of GNSS constellations – GPS, GLONASS, Galileo and Compass.

As explained in chapter 6, different GNSS systems use different reference frames and different reference time scales for their positioning and timing solution. Therefore for each system, a matrix transforming satellite coordinates of a given GNSS system into the mapping coordinates has to be performed.

Depending on the availability of known positions of satellites obtained from navigation messages of different GNSS systems, the multipath signal propagation model is evaluated.

Test measurements were performed in Europe and Asia for GPS, GLONASS, Galileo and Compass. With the fact that the evaluation of the ray-tracing method and simulations is the same for all GNSS systems, further conclusions are concentrated on the GPS, which is the most available GNSS system.

SIMULATION EXAMPLE

Model 1: Europe, Prague, Studentská street

A – Model preparation

A building block in city model of Prague with variable parameters for street width, street length, and building block parameters with an assumed position of the receiver (50°06’10.01” N, 14°23’24.18” E) was considered.

Figure 15. 1 shows a street as captured in Google Earth, Figure 15. 2 shows the user view of the same street.

The selected urban environment is captured by 3D Ripper DX and imported into Autodesk 3ds Max 2011 - the geometry data of the street is then exported into .obj file, as described in chapter 11 (Figure 15. 3 shows the Studentská street in .obj file).

Figure 15. 1 Street model of Prague in Google Earth

Figure 15. 2 Snapshot of the user view in Google Earth

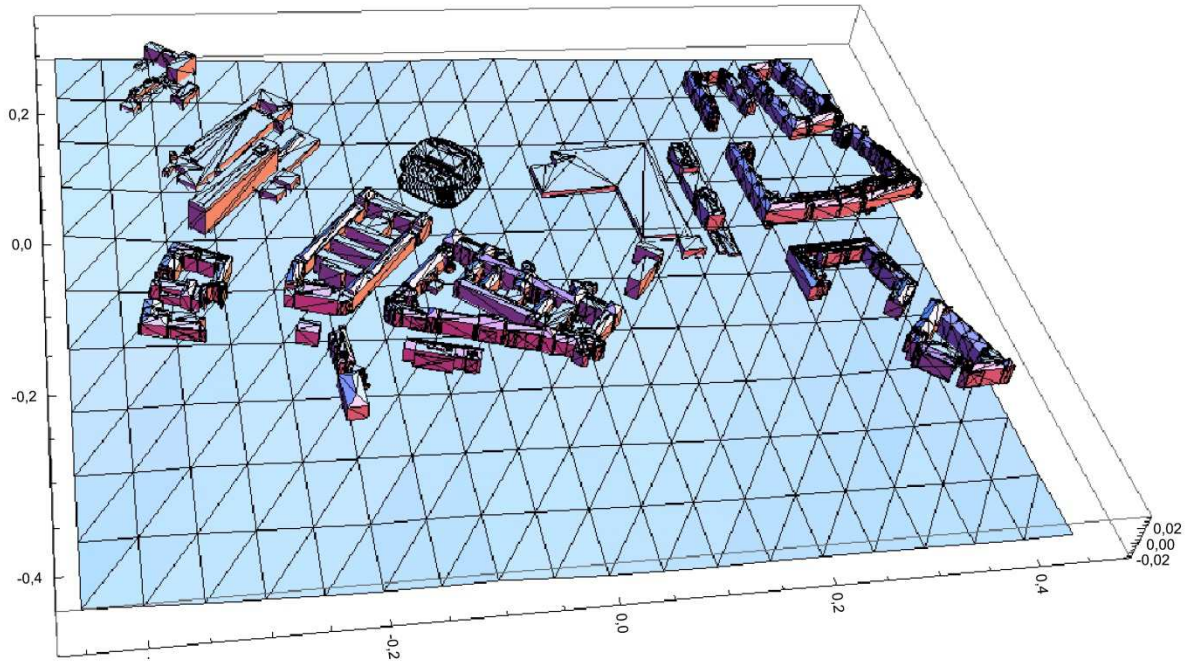

Figure 15. 3 Street model of Prague in .obj file

The building (or street) layout is made up of triangles ABC which are imported into Matlab in the form of .cvs files. In the Table 15. 1 below, examples of triangle coordinates of Studentská street are shown.

Ax	Ay	Az	Bx	By	Bz	Cx	Cy	Cz
-0.1086	-0.0365	0.0046	-0.0595	0.0397	0.0076	-0.1086	0.0397	0.0066
-0.1577	-0.0365	0.0036	-0.1086	-0.0365	0.0046	-0.1086	0.0397	0.0066
-0.1531	-0.0749	0.0032	-0.1553	-0.0809	0.003	-0.1553	-0.0809	-0.0112
-0.1531	-0.0749	-0.0119	-0.1531	-0.0749	0.0032	-0.1553	-0.0809	-0.0112
-0.1471	-0.083	-0.0148	-0.1503	-0.0759	-0.0148	-0.1503	-0.0759	-0.0132
-0.1466	-0.084	-0.0151	-0.1466	-0.084	-0.0148	-0.1471	-0.083	-0.0148
-0.1512	-0.0845	-0.0131	-0.1466	-0.084	-0.0148	-0.1466	-0.084	-0.0151
-0.1544	-0.0848	-0.0118	-0.1544	-0.0848	-0.0119	-0.1512	-0.0845	-0.0131
-0.1553	-0.0809	0.003	-0.1544	-0.0848	0.0031	-0.1544	-0.0848	-0.0118
-0.1553	-0.0809	-0.0112	-0.1553	-0.0809	0.003	-0.1544	-0.0848	-0.0118

Table 15. 1 Examples of triangle coordinates, Studentská Street, Prague

Navigation message extraction to obtain satellites coordinates (Table 15. 2) and their transfer into mapping coordinates is done next, chapter 11.

SV Id	x-axis (km)	y-axis (km)	z-axis (km)
1	-13588.73232	22126.95751	5159.55872
2	16473.62587	-1019.706207	-20413.98619
3	-17858.54625	1989.119793	19045.993112
4	4294.169786	20627.36973	-16296.31843
5	26516.42648	-1724.239163	-2094.132017
7	-5040.233095	24550.11494	8313.92523
8	-1615.864928	21746.78234	14861.25097
10	19225.8567	9773.088664	-16112.9303
11	-12612.00182	18505.91483	13635.79484
12	19520.01957	-10914.42024	-14230.10818
13	412.805326	21464.23002	-15646.40288
14	-14368.52792	-22436.53239	-153.971863
15	13415.90698	-8351.429262	21305.04378
16	-26689.41852	264.574192	-1955.026965
17	15020.73895	22053.55197	-14.66304
18	-1464.07134	-16138.46335	21502.42862
19	-15045.77168	3773.496533	21456.36224
20	-15641.07272	14831.28911	-15664.15884
21	-20.861492	-23610.36496	12360.08982
22	-15595.47029	-11897.4409	18197.17813
23	-7315.205188	14841.62373	-20570.04876
24	15175.25396	-19731.51591	9106.708229
25	7490.179983	-14970.10852	-20665.35528
26	17843.3309	5474.078867	18355.51797
27	-19505.98	-6566.391408	16812.13716
28	10845.36831	13278.35981	20927.5264
29	-1573.950303	-21502.30104	-15510.93115
30	2380.568566	20550.59282	16626.24589
31	-11593.58282	-9662.995279	-21672.00008
32	-24825.38928	5528.768941	-6548.814559

Table 15.2 Examples of satellite coordinates obtained from the navigation message (1.12.2014 – 6pm)

B – Detection of GNSS signals propagation

The model described in previous section is evaluated using the multipath detection algorithm based on an assumed position of the receiver, digital 3D maps information, and known positions of GNSS satellites, chapter 12.

As a result, a list of all direct paths and possible reflections examples for a given satellite and the receiver along with coordinate data of reflected points is displayed – i.e. three examples below:

Table 15. 3 shows the result of two reflections.

Satellite ID 7	
Direct Path:	No
Number of signals with a single reflection:	0
Number of signals with two reflections:	3
Signal 1	
Reflection point coordinate data (X1m, Y1m, Z1m):	1.0e+011 * [3.7131, -1.9701, 0.1399]
Reflection point coordinate data (X2m, Y2m, Z2m):	1.0e+002 * [-1.5763, -0.7414, -0.0099]
Signal 2	
Reflection point coordinate data (X1m, Y1m, Z1m):	1.0e+007 * [2.0910, -1.1095, 0.2041]
Reflection point coordinate data (X2m, Y2m, Z2m):	1.0e+012 * [-5.4743, -6.2745, -0.7086]
Signal 3	
Reflection point coordinate data (X1m, Y1m, Z1m):	1.0e+002 * [-1.4315, -0.6138, -0.0076]
Reflection point coordinate data (X2m, Y2m, Z2m):	1.0e+002 * [-1.4427, -0.5883, -0.0084]

Table 15. 3 Results shown for GPS, Satellite ID 7

Table 15. 4 shows possible signal propagation for satellite ID 19.

Satellite ID 19	
Direct Path:	Yes
Total Distance	25362443 meters
Direct Path:	No
Number of signals with a single reflection:	1
Signal 1	
Reflection point coordinate data (X1m, Y1m, Z1m):	-176.1279 -57.3158 -4.2000
Total Distance	25362588 meters
Direct Path:	No
Number of signals with a single reflection:	2
Signal 1	
Reflection point coordinate data (X1m, Y1m, Z1m):	1.0e+002 * [-1.2264 + 0.0000i 0.0602 + 0.0000i -0.0543 - 0.0000i]
Total Distance	25362516 meters
Signal 2	
Reflection point coordinate data (X1m, Y1m, Z1m):	-123.6280 2.6842 -4.2000
Total Distance	25362516 meters

Table 15. 4 Results shown for GPS, Satellite ID 19

Table 15. 5 shows the result of one reflection.

Satellite ID 5	
Direct Path:	No
Number of signals with a single reflection:	1
Reflection point coordinate data (Xm, Ym, Zm):	1.0e+002 * [-1.8066, -0.6410, -0.0499]

Table 15. 5 Results shown for GPS, Satellite ID 5

From the knowledge of reflection points coordinates, the distance from the satellite to the receiver is computed, equation (12. 19), equation (12. 22). Computation time increases extensively with the amount of 3D map information, and number of satellites and receivers.

C – Detection of the User's Pseudo-Position

Computed data are forwarded to the receiver - based on the results of the ray-tracing algorithm, the receiver computes its new position which is different from the originally known position of the user.

Depending on the difference between the position computed and data measured, a consequent decision which half of the route is relevant, moving the next step of the computation to the midpoint of this segment.

Another round of signal computation for the new position is done until the difference between the measured and computed position lies within the desired tolerance interval. The last computed position is the actual position.

These steps account for standard engineering tasks. It is true that this sort of computation is dependent on considerable computing power: The completion of the above mentioned calculation may require up to several hours of time using a standard PC. However, the necessary solution does not require having this kind of computer power on the spot or waiting until the processors capable of this output are available: The data may be sent to the cloud via a line of communication where this sort of power may be at hand.

The dissertation research also constitutes the material for the patent application entitled "Method of determining the actual position of a user of the GNSS in complicated environments and a system for implementing this method."

16 CONCLUSION

The presence of reflected and diffracted signals in urban environments seriously degrades GNSS positioning in terms of accuracy, integrity, and precision. Possible combinations of GNSS constellations promise better results with respect to GPS only. Although the current situation only allows using GPS and GLONASS to the full extent, additional satellites of Galileo and Compass will offer significantly improved GNSS performance and availability in the near future.

Different techniques exist to mitigate the effect of multipath signals. Methods based on so-called Maximum Likehood Estimation (MLE) are being tested, such as Multipath Estimation Delay Lock Loop (MEDLL), Fast Iterative Maximum-Likelihood Algorithm (FIMLA), Multipath Mitigation Technology (MMT), and Vision Correlator (VC) among others. Nonetheless, methods of this sort are very demanding mathematically so it is very difficult to implement them. All these methods discovered so far do show some results but remain inadequate for the time being. Moreover, these procedures usually demand the use of highly specialized, high-cost, relatively low-efficient receivers.

Within this research, a new ray-tracing model for simulation of GNSS signals reception in urban canyons was designed. To investigate whether GNSS signals have arrived at a receiver directly or through reflections, the ray-tracing algorithm was introduced based on information obtained from 3D buildings model, assumed position of the receiver, and known position of GNSS satellites extracted from the navigation message.

There is no direct way to export the geometry with textures and coordinates mapped automatically. Therefore a new technique to model complex environments using an intelligent map was defined and derived.

For each satellite, the algorithm determines whether the signal has arrived at the receiver through a direct path or through multipath reflections. Furthermore, the algorithm is able to estimate the number of multipath reflections and their coordinate data within the proposed simulation system. With this information, the distance the signal travelled to the receiver, as well as its the transit time, are calculated.

The model is established and validated using experimental as well as real data. It is specially designed for complex environments and situations where positioning with highest accuracy is required – a typical example is navigation for the visually impaired.

This approach can be then used to determine the user's position in dynamic propagation environment thanks to the fact that if it is possible to calculate the total propagation path length of the GNSS signals – using intelligent maps and other data – then it is also possible

to perform the order of operations in reverse and thus to determine the actual, unknown position of the user.

Based on the research results presented in this work, detection of GNSS signals propagation in urban environments can improve accuracy of the pedestrian positioning. The data processing algorithm requires sufficient computational power. Therefore, it is expected the data will be sent to the cloud for faster computation.

In future work, an investigation in the multi-constellation GNSS area and right selection of direct/multipath signals using the method presented, combined with other options – e.g. using antennas capable of receiving only phase undistorted GNSS signals, or cameras able to determine which part of the sky is uninterrupted by objects – seems to be interesting.

APPENDIX

Appendix 1 Content of the attached CD

Name	Function
3d_data_retrieval	loading geometry data from GE in the form of polygons
binary_search_test	actual user position in urban environments determination
distance	distance between two points computation
distance_with_one_point_of_reflection	final distance with one reflection point computation
distance_with_two_points_of_reflection	final distance with two reflection points computation
false_position	wrong user position identification
five_points_of_reflection	five points of reflection and their coordinates computation
four_points_of_reflection	four points of reflection and their coordinates computation
half-interval search algorithm	final position of the user computation
intersection_of_point_and_plane	intersection of a point and a plane determination
line	line between two points, used for illustration
line_of_sight	line of sight between two points determination
obstruction_in_view	linearly independent vectors estimation
one_point_of_reflection	single reflection point and its coordinates computation
pseudoranges_computation	ray-tracing model evaluation; pseudoranges computation
satellites	loading satellites coorinates from navigation message
satellite_coordinates	transformation of coordinates matrix
single_reflection_path	single reflection between two points determination
three_points_of_reflection	three points of reflection; their coordinates computation
trilateration	trilateration calculation
two_points_of_reflection	two points of reflection and their coordinates computation
two_reflections_path	two reflections between two points determination

Table A Matlab scripts description

Appendix 2 MATLAB code on the supplemented CD attached to the inside back cover.

BIBLIOGRAPHY

[1] Hornbostel, A. *Propagation Problems in Satellite Navigation*. DLR, Institute of Communications and Navigation. Proceedings of WFMN07, Chemnitz, Germany [online]. WFMN07_II_A1, pp. 42-49.

[2] Misra, P. and P. Enge. *Global Positioning System: Signals, Measurements and Performance.*2nd ed. Lincoln, MA: Ganga-Jamuna Press, 2006. ISBN 0-9709544-1-7.

[3] Petovello, M.and P. Groves. *Multipath vs. NLOS signals.* InsideGNSS [online]. GNSS Solutions, November/December 2013.

[4] Sahmoudi, M. Landry, R. *Probabilities and Multipath. Mitigation Techniques Using Maximum-Likelihood Principles.* InsideGNSS [online]. Technical Article, November/December 2008.

[5] GROVES, P. D. *Principles of GNSS, Inertial, and Multi-Sensor Integrated Navigation Systems (GNSS Technology and Applications).* 2nd ed. Boston: Artech House, 2013. ISBN 978-1-60807-005-3.

[6] Groves, P. D., Z. Jiang, M. Rudi, P. Strode. *A Portfolio Approach to NLOS and Multipath Mitigation in Dense Urban Areas.* Proceedings of the 26th International Technical Meeting of The Satellite Division of the Institute of Navigation (ION GNSS 2013*)*. (pp.3231-3247). Manassas,US The Institute of Navigation, 2013.

[7] Grewal, M.S., L.R. Weil and A.P. Andrews. *Global Positioning Systems, Inertial Navigation, and Integration*. John Wiley & Sons, Inc., 2007, pp. 144-194, ISBN-13 978-0-470-04190-1.

[8] Lau, L. and P. Cross. *Investigations into Phase Multipath Mitigation Techniques for High Precision Positioning in Difficult Environments.* Journal of Navigation, 2007, Vol. 60, No. 1, pp. 95−105.

[9] Kaplan, E.D and Ch. J. Hegarty. *Understanding GPS - Principles and Applications*. 2nd ed. Artech House, 1996. ISBN 0-89006-793-7.

[10] Miller-Jones, Edward R. *Global Navigation Satellite Systems.* Fastbook Publishing, 2011. ISBN 9786130113483.

[11] *Official U.S. Government information about the Global Positioning System (GPS) and related topics.* October 2014 [online]. Available: http://www.gps.gov/

[12] Dana, Peter H. *Global Positioning System Overview.* The Geographer's Craft Project,

Department of Geography, the University of Colorado at Boulder, 1999.

[13] Borre, K., D. M. Akos, N. Bertelsen, P. Rinder and S. H. Jensen. *A Software-Defined GPS and Galileo Receiver. A Single-Frequency Approach.* Series: Applied and Numerical Harmonic Analysis. Boston: Birkhäuser, 2007. ISBN 978-0-8176-4540-3.

[14] *High Accuracy GNSS Solutions and Services*. October 2014 [online]. Available: http://www.positim.com/gps_overview.html

[15] Gleason, S. and D. Gebre-Egziabher. *GNSS Applications and methods*. Artech House, 2009. ISBN 978-1-59693-329-3.

[16] *GPS signals (L1, L2, L5).* December 2014 [online]. Available: http://geoconnect.com.au

[17] Wells, D.E., N. Beck, D. Delikaraoglou, A. Kleusberg, E.J. Krakiwsky, G. Lachapelle, R.B. Langley, M. Nakiboglu, K.P. Schwarz, J.M. Tranquilla and P. Vaníček (1986). *Guide to GPS Positioning.* Canadian GPS Associates, Fredericton, N.B., Canada.

[18] *GNSS Technologies and Receiver Testing.* Agilent Technologies, Inc. Published in USA, 2013. 5991-2288EN.

[19] *Federal Space Agency Information-analytical centre.* September 2014 [online]. Available: http://www.glonass-center.ru/en/

[20] Abbasiannik, S. *Multichannel Dual Frequency GLONASS Software Receiver in Combination with GPS L1 C/A.* (M.Sc. thesis). Department of Geomatics Engineering, University of Calgary, Alberta, 2009. UCGE Report 20286.

[21] *GLONASS ICD.* Global Navigation Satellite System GLONASS: Interface Control Document. Coordination Scientific Information Center, Moscow, 1998.

[22] European Space Agency: *Galileo*. Fact Sheet. December 2013 [online]. Available: http://www.esa.int/ESA

[23] *Global Navigation Satellite System (GNSS)* [online]. Available: https://www.princeton.edu/~alaink/Orf467F07/GNSS.pdf

[24] Hein,G.W., J. Godet, J.-L. Issler, J.-Ch. Martin, R. Lucas-Rodriguez and T. Pratt. *The GALILEO Frequency Structure and Signal Design.* Members of the Galileo Signal Task Force of the European Commission, Brussels [online]. Available: http://www2.ulg.ac.be/ipne/garnir/time/galileo/gal_stf_final_paper.pdf

[25] Richharia, M. and L. D. Westbrook. *Satellite Systems for Personal Applications: Concepts and Technology.* John Wiley & Sons Ltd, 2010. ISBN: 978-0-470-71428-7.

[26] European Union, *European GNSS (Galileo) Open Service. Signal in Space Interface*

Control Document. Ref : OS SIS ICD, Issue 1.1. September, 2010.

[27] BeiDou Navigation Satellite System, *Signal In Space Interface Control Document. Open Service Signal (Version 2.0).* China Satellite Navigation Office. December, 2013.

[28] BeiDou Navigation Satellite System, *Report on the Development of BeiDou Navigation satellite System (Version 2.1).* China Satellite Navigation Office. December, 2012.

[29] Gao, Xingxin G., A. Chen, S. Lo, D. De Lorenzo, T. Walter, and P. Enge. *Compass-M1 Broadcast Codes in E2, E5b, and E6 Frequency Bands.* IEEE J. Sel. Topics in signal Processing, vol. 3, no. 4, August 2009.

[30] ICAO, International Civil Aviation Organization. *Global Navigation satellite System (GNSS) Manual.* Document 9849 AN/457. 1st ed., 2005.

[31] EGNOS: *Discover EGNOS, Existing SBAS.* November 2014 [online]. Available: http://egnos-portal.gsa.europa.eu/discover-egnos/about-egnos/what-sbas.

[32] European Space Agency: *EGNOS*. December 2013 [online]. Available: http://www.esa.int/Our_Activities/Navigation/The_present_-_EGNOS/What_is_EGNOS

[33] EGNOS Service Provider: *EGNOS system description*. October 2014 [online]. Available: http://www.essp-sas.eu/egnos_system_description

[34] Brocard, D., T. Maier and C. Busquet. *EGNOS Ranging and Integrity Monitoring Stations (RIMS).*2003, ESA [online]. Available: http://www.egnos pro.esa.int/Publications/GNSS%202000/GNSS2000_rims.pdf

[35] Parkinson, B. W. and J. J. Spilker. *Global Positioning System: Theory and Applications Volume 2 (Progress in Astronautics and Aeronautics).* Washington, DC: American Institute of Aeronautics and Astronautics, 1996. ISBN 1-56347-107-8.

[36] Javier, F. and G. Martinez. *Performance of new GNSS satellite clocks.* Karlsruher Institut für Technologie, 2014. ISBN 9783731501121.

[37] National Geospatial-Intelligence Agency: *World Geodetic System 1984.* October 2014 [online]. Available: http://www.unoosa.org/pdf/icg/2012/template/WGS_84.pdf

[38] National Imagery and Mapping Agency. *Department of Defense World Geodetic System 1984: Its Definition and Relationships with Local Geodetic Systems.* NIMA TR83502. Bethesda, MD, 2000.

[39] JiunHan Keong. *GPS/GLONASS Attitude Determination with a Common Clock using a Single Difference Approach.* ION GPS99 Conference. Department of Geomatics Engineering, University of Calgary, Canada, 1999.

[40] Gendt, G., Z. Altamimi, R. Dach, W. Sohne, T. Springer. *GGSP: Realization and maintenence of the Galileo Terrestrial Reference Frame.* Padua, Italy, 2009.

[41] European Space Agency: *Galileo Science Opportunity Document.* Version 2.0, April 2010 [online]. Available: http://egep.esa.int/egep_public/file/GSOD_v2_0.pdf

[42] Yang, Y. and J. Tang. *COMPASS/BeiDou Coordinate and Time Reference Systems.* Global Navigation Satellite Systems: Report of a Joint Workshop of the National Academy of Engineering and the Chinese Academy of Engineering 2012.

[43] *The Future of Leap Seconds.* January 2015 [online]. Available: http://www.ucolick.org/~sla/leapsecs/onlinebib.html

[44] Lewandowski, W. *Global navigation satellite systems and their system times.* International Bureau of Weights and Measures. January 2015 [online]. Available: https://itunews.itu.int/en/4272-Global-navigation-satellite-systems-and-their-system-times.note.aspx

[45] Fleisch, D. *A Student's Guide to Maxwell's Equations*. 1st ed. Cambridge University Press, 2008. ISBN 978-0521701471.

[46] Becherrawy, T. *Electromagnetism: Maxwell Equations, Wave Propagation and Emission.* Wiley-ISTE, June 2012. ISBN: 978-1-84821-355-5.

[47] Orfanidis, S. J. *Electromagnetic Waves and Antennas.* Rutgers University, 2002 [online]. ISBN 0130938556. Available: http://www.ece.rutgers.edu/~orfanidi/ewa/

[48] Torre, CH. G. *20 Polarization*. 2014. Foundation of Wave Phenomena. Book 3. http://digitalcommons.usu.edu/cgi/viewcontent.cgi?article=1020&context=foundation_wave

[49] Fitzpatrick, R. *Geometric Optics*. June 2007 [online]. Available: http://farside.ph.utexas.edu/teaching/302l/lectures/node123.

[50] *The Feynman Lectures on Physics, Volume I* [online]. 2013 Interference. Diffraction. Radiation Damping. Light Scattering. Polarization. Modes. Available at: http://www.feynmanlectures.caltech.edu/.

[51] Ebner, A. *On the attainable accuracy of multi-system GNSS positioning in high-multipath urban environments*, Master Thesis, University of Graz, 2008.

[52] Braach, M: *On the Characterization of Multipath in Satellite-Based Precision Approach and Landing Systems*, PhD Dissertation, Department of Electrical and Computer Engineering, Ohio University, Athens, OH, June 1992.

[53] Petrovski, I.G., T. Tsujii: *Digital Satellite Navigation and Geophysics, A Practical Guide with GNSS Signal Simulator and Receiver Laboratory.* Cambridge University Press, 2012. ISBN 9780521760546.

[54] Petovello, M.G. *Fundamentals of Fundamentals of GNSS Receivers. 2nd* BEIDOU/GNSS Summer School on GNSS Frontier Technology. Beihang University, August 2013.

[55] Tsui, J. B. Y. *Fundamentals of Global Positioning System Receivers: A Software Approach.* John Wiley & Sons, Inc., New York, 2000. ISBN 0-471-38154-3.

[56] Akos, D. M. *A Software Radio Approach to Global Navigation Satellite System Receiver Design.* Ph.D. thesis, Ohio University, Athens, OH, 1997.

[57] Borre, K. and G. Strang. *Algorithms for Global Positioning.* Wellesley-Cambridge Press, Wellesley, MA, 2012. ISBN 978-0-9802327-3-8.

[58] Parkinson, B.W. and J. J. Spilker. *Global Positioning System: Theory and Applications Volume 1 (Progress in Astronautics and Aeronautics).* Washington, DC: American Institute of Aeronautics and Astronautics, 1996. ISBN 1-56347-106-X.

[59] Brenner C. *Building reconstruction from images and laser scanning.* Inter. J. Appl. Earth Obs. Geoinf. 2005; 6:187–198.

[60] Umesh Chandra Pati. 3-*D Surface Geometry and Reconstruction: Developing Concepts and Applications,* (National Institute of Technology, Rourkela, India), Publisher: IGI Global; 1 edition (February 29, 2012), ISBN-10: 1466601132.

[61] Neutens, T. and P. De Maeyer. *Developments in 3D Geo-Information Sciences*. Springer, Berlin, 2010. ISBN 978-3-642-04790-9.

[62] IGS Product Availability: *GPS ephemeris, clock and earth orientation solutions.* 2014 [online]. Available: http://igscb.jpl.nasa.gov/components/prods_cb.html

[63] Leduc, S. A. *Linear Algebra* (Cliffs Quick Review), Cliffs Notes, 1996 [online]. ISBN 978-0-8220-5331-6. Available: http://www.cliffsnotes.com/math/algebra/linear-algebra/real-euclidean-vector-spaces/linear-independence

[64] Sunday, D. *About Planes and Distance of a Point to a Plane.* 2001 [online]. Available: http://www.geometry algorithms.com

[65] Pany, T. *Navigation Signal Processing for GNSS Software Receivers.* Norwood, MA: Artech House, 2010. ISBN 978-1-60807-027-5.

[66] Prasad, R. and M. Ruggieri. *Applied Satellite Navigation Using GPS, GALILEO and*

Augmentation Systems. Boston: Artech House, 2005. ISBN 1-58053-814-2.

[67] El-Rabbany, A. *Introduction to GPS. The Global Positioning System.* 2nd ed. Norwood, MA: Artech House, 2006. ISBN 978-1-59693-016-2.

[68] Knuth, D. The Art of Computer Programming: *Sorting and Searching* (3rd ed.), Addison-Wesley, 1997. ISBN 0-201-89685-0. Section 6.2.1: Searching an Ordered Table, pp. 409–426.

Software

[S1] Google Earth (Google).
URL: **http://earth.google.com**

[S2] 3D Ripper DX v1.8 (Roman Lut).
URL: **http://3d-ripper-dx.software.informer.com**

[S3] Autodesk 3ds Max 2011 (Autodesk).
URL: **http://www.autodesk.com/education/free-software/3ds-max**

[S4] Matlab 7.11.0 (Mathworks).
URL: **http://www.mathworks.com/**

[S5] Mathematica 8 (Wolfram)
URL: **http://www.wolfram.com/products/?source=nav**

PUBLICATIONS

1. Publications related to thesis

Journals (Impact)

None

Journals (Reviewed)

Planned:

- Pisova, P., Chod, J.: Detection of GNSS signals propagation in urban canyons using 3D city models. In *Advances in Electrical and Electronic Engineering*. Article will be published within the next issue (March 2015).

Patent

- Pisova, P., Chod, J.: Patent application PV 2015: "Způsob stanovení skutečné polohy uživatele GNSS ve složitém prostředí a systém k provádění tohoto způsobu" (in Czech). "Method of determining the actual position of a user of the GNSS in complicated environments and a system for implementing this method" (in English).

Conference Proceedings

- Chod, J., Píšová, P., Koláčný, R., Šafránek, M.: HW a SW of the Navigation Centre for Blind Persons. In *Sborník přednášek konference NavAge 08.* Praha: Technology&Prosperity, 2008. ISBN 978-80-87205-00-6.

- Chod, J., Píšová, P., Šafránek, M.: Navigace nevidomých – 2008. *EMTECH 2008.* Praha: ČVUT v Praze, FEL, 2008. ISBN 978-80-01-04198-7.

- Chod, J., Píšová, P., Šafránek, M., Koláčný, R.: Projekt navigace nevidomých – 2008. *MonAMI* - IST – 5 – 035147. Košice: Technical University of Košice, 2008.

- Píšová, P.: Global Navigation Satellite Systems for Mobile Communication. In *Applied Electronic 2010.* Pilsen: University of West Bohemia, 2010, p. 261-264. ISSN 1803-7232. ISBN 978-80-7043-865-7.

- Píšová, P., Kalfus, R., Chod, J.: Detection of Reflected GPS Signals. In *13th International Conference on Research in Telecommunication Technologies 2011*. Brno: Vysoké učení technické v Brně, Fakulta elektrotechniky a komunikačních technologií, 2011, p. II-35-II-39. ISBN 978-80- 214-4283-2.

Grants

- Chod, J.: Innovation of Laboratory Projects Assignments for the Subject MKS. 08--08, FRV 2294 F1a, 2008.

- Píšová, P.: Modernization of Laboratory Exercises in the Field of Navigation Systems. 11--11, FRV G1 2107, 2011.

- Chod, J.: Advanced Navigation of the Blind.13--15, TA03011396, 2014.

2. Other publications

Journals (Impact)

None

Journals (Reviewed)

None

Conference Proceedings

- Vojtěch, L., Píšová, P.: RFID - A Technology for Radio Frequency Contactless Identification. In *Moderní trendy v digitálních přenosových systémech*. Praha: Česká elektrotechnická společnost, 2007, s. 39-42. ISBN 978-80-02-01922-0.

- Píšová, P. - Tomešová, K. - Plotnikova, M. - Zikmund, M.: Communication and Nanotechnology. In *13th International Student Conference on Electrical Engineering*. Prague: CTU, Faculty of Electrical Engineering, 2009, p. C6.

Grants

- Krejčí, J.: Suitable Methods for Evaluation of Image Signal Quality in Digital TV Systems. 09--09, FRV 1378G1, 2009.

- Šafránek, M.: Innovation of Laboratory Exercises in the Subject 'Switching Systems'. 10--10, FRV G1 2219, 2010.

- Šafránek, M.: Communication and automatic data collecting system with a use of satellite network, high reliability and low power consumption for Czech Antarctic base station. 10--11, SGS SGS10/183/OHK3/2T/13, 2010.

- Zeman, T.: Modern Coding Methods. 10--10, FRV F1a 1752, 2010.